LOW CARBON LIVING CRC

# RP1014: Impact of energy efficient pool pumps on peak demand, energy costs and carbon reduction

Final Report

| | |
|---|---|
| Authors | Dr Jianzhou Zhao; Dr Jose Bilbao; Mr Ted Spooner; Professor Alistair Sproul |
| Title | RP1014: Impact of energy efficient pool pumps on peak demand, energy costs and carbon reduction Final Report |
| ISBN | |
| Date | April 30, 2019 |
| Keywords | Swimming pool filtering; Solar pool heating; High-efficiency water pumping; Whole system approach |
| Publisher | |
| Preferred citation | |

Australian Government
Department of Industry, Innovation and Science

Business Cooperative Research Centres Programme

## Acknowledgements

This research is funded by the CRC for Low Carbon Living Ltd supported by the Cooperative Research Centres program, an Australian Government initiative

## Disclaimer

Any opinions expressed in this document are those of the authors. They do not purport to reflect the opinions or views of the CRCLCL or its partners, agents or employees.

The CRCLCL gives no warranty or assurance, and makes no representation as to the accuracy or reliability of any information or advice contained in this document, or that it is suitable for any intended use. The CRCLCL, its partners, agents and employees, disclaim any and all liability for any errors or omissions or in respect of anything or the consequences of anything done or omitted to be done in reliance upon the whole or any part of this document.

## Peer Review Statement

The CRCLCL recognises the value of knowledge exchange and the importance of objective peer review. It is committed to encouraging and supporting its research teams in this regard.

The author(s) confirm(s) that this document has been reviewed and approved by the project's steering committee and by its program leader. These reviewers evaluated its:

- originality
- methodology
- rigour
- compliance with ethical guidelines
- conclusions against results
- conformity with the principles of the Australian Code for the Responsible Conduct of Research (NHMRC 2007),

and provided constructive feedback which was considered and addressed by the author(s).

# Contents

# Executive Summary

## 1. Energy efficient residential swimming pool filtering systems

- The whole system approach was adopted to optimize a residential pool filtering system. The project presents for the first time, the experimental measurements of the pool water quality (i.e., the chemical concentrations) and all energy-consuming components when operating the filtering system at low flow conditions;
- A Business as Usual (BAU) residential pool filtering system usually operates at a water flow rate of approximately 3.7 L/s (the highest pump speed of 2850 RPM) and uses about 5.5 kWh of electricity per day (37,500 litre pool, 1 tunrover in 2.8 h);
- A typical salt water chlorinator and a pressure pool auto-cleaner did not work well for flow rates of less than 1.0 L/s and 1.3 L/s respectively, i.e., the chlorinator shut off whilst the pressure auto-cleaner lost movability, resulting in a turbid pool with an accumulation of debris;
- Operating at a flow rate of 1.7 L/s achieved the optimal energy efficiency for a residential pool filtering system with a pressure auto-cleaner in use. The daily energy use was 1.8 kWh per day, which represented an energy saving of approximately 70% when compared to the BAU high-speed pool filtering scenario. The turnover time was 8.2 h.
- With a robotic pool cleaner retrofitted, the residential pool filtering system could run at an even lower, optimal flow rate of 1 L/s and consumed 1.5 kWh of electricity per day with a turnover time of 14 h. This not only achieved further energy saving in comparison to the filtering system with the pressure auto-cleaner in use, in addition more effective pool circulation and skimming was also achieved, resulting in improved pool cleanliness.
- Whe powering the system using Photovltiacs, it is cost-effective to use a typical 2 kW PV system to supply the required pump load of an energy efficient residential pool filtering system for Sydney, Melbourne, and Brisbane climates. Assuming all the PV electricity was self-consumed, the PV-powered filtering systems using either a pressure auto-cleaner or a robotic cleaner would achieve attractive payback periods of less than 5.5 years.

The full conference paper, describing the work relating to the energy efficient pool filtering system, is attached as an appendix to this report (Appendix 1).

## 2. Energy efficient residential solar pool heating systems

- Operating the pool filtering systems under low flow conditions can deliver significant pump energy saving. However, to date in Australia, this approach has not been widely applied to residential solar pool heating systems.
- This project addressed the fundamental hydraulic theory of typical residential solar pool heating systems, based on which, the minimum required pressure by the solar pump to maintain a proper operation (i.e., the vacuum relief valve stays closed) can be determined. The minimum pump pressure ($\Delta P_{pump}$) is given by:

$$\Delta P_{pump} > \Delta P_{1-2} + \rho_w g H + \frac{1}{2}\rho_w V_{av}^2$$

  where $\Delta P_{pool\_vac}$ is the pressure loss from the pool skimmer box to the vacuum relief valve; $\rho_w$ is the density of water; $H$ is the height of the vacuum relief valve above the pool water level; and $V_{av}$ is the average velocity of the water in the pipe at the location of the vacuum valve.
- The project presents for the first time, the experimental results obtained using a commercially available multi-speed pool pump (default speeds of 2000, 2410, and 2850 RPM) to operate a residential solar pool heating system under low flow and low-pressure conditions. The system consisted of a 15 m by 1.4 m unglazed, plastic tube solar thermal collector and a 36 m$^2$ in-ground, open-air swimming pool, located in Sydney.
- Experimental results were used to validate a theoretical model for the collector and the pool, which achieved the best overall fitting results (an *MBE* close to zero and an $R^2$ greater than 95%) for both the rate of heat output and the outlet water temperature. The validated model was used to simulate the whole of system performance under various scenarios.
- Typical solar pool heating system utilises a pump that consumes ~750 W or more and 6 kWh/day of electricity. For the high-speed BAU scenario investigated in this project, the multi-speed pump was operating at the high-speed setting and the mass flow rate per unit collector area ($\dot{m}/A_c$) was 0.076 kg/s/m$^{-2}$. The corresponding pump pressure was 144 kPa.
- Experimental results showed that closing a throttle valve (located downstream of the vacuum relief valve) ensured that the pressure of the pump was high enough to keep the vacuum relief valve remained closed at all times.
- Experimental and modelled results showed that operating the system at the lowest pump speed (2000 RPM) and a low $\dot{m}/A_c$ of 0.016 kgs$^{-1}$m$^{-2}$ achieved the optimal energy efficiency. The pump pressure was 79 kPa at such a low flow and due to the significant reduction in the pump pressure (from 144 to 79 kPa), the optimal scenario delivered pump energy savings of approximately 60% when compared to the high-speed BAU operation. The optimal value of $\dot{m}/A_c$ is equal to around 20% of the BAU value of 0.076 kg/s/m$^{-2}$ and below the lower limit specified by the International and Australian Standards of 0.03 kg/s/m$^{-2}$.
- This approach also increased the system coefficient of performance (*COP*) by 2.5 times whilst only marginally reducing the thermal performance of the system. Modelling results under the Sydney climate showed that similar thermal performance could be achieved with either a) 1.3 hours longer pump running time per day or b) an approximately 15% increase of the collector area with similar pump running times.

- Assuming all residential solar pool heating systems in Australia were operated at a lower flow rate and with a low energy pump, approximately 180 GWh of electricity could be saved every year, which corresponds to approximately 150 kt $CO_2$-e of GHG emission reductions.
- Further experimental work was carried out to operate a residential solar pool heating system with a correctly sized high-efficiency water pump. At the optimal $\dot{m}/A_c$ of 0.016 $kgs^{-1}m^{-2}$, the pump power was only 0.125 kW and for similar pool thermal performance, the modelling results showed pump energy reduction of approximately 80% when comparing to the BAU operation at 0.076 $kg/s/m^{-2}$. The COP has increased drastically to 85 and cost savings of ~AU$200 could be realized per year. The high-efficiency solar pool heating pump retrofit has a payback period of around 3.3 years.

The full journal article, describing the work relating to the high efficiency solar pool heating system, is attached as an appendix to this report (Appendix 2).

# Appendix 1

## Whole System Design of an Energy Efficient Residential Pool System

**Jianzhou Zhao[1], Jose I. Bilbao[1], Edward D. Spooner[2] and Alistair B. Sproul[1]**

[1] *School of Photovoltaic and Renewable Energy Engineering, UNSW, Sydney (Australia)*

[2] *School of Electrical Engineering and Telecommunications, UNSW, Sydney (Australia)*

**Abstract**

The impact of low-speed filtration on the performance of salt water chlorinators, pool cleaners, and the pool water quality, based on experimental and modelled data, is investigated. Results show that a typical salt water chlorinator and pressure pool cleaner do not work well for flow rates of less than 1 litre $s^{-1}$ and 1.3 litre $s^{-1}$ respectively. With the implementation of a robotic pool cleaner, energy savings of more than 70% can be obtained by operating the filtration system at around 1 litre $s^{-1}$ with a correctly adjusted chlorinator setting. This does not compromise the system performance and achieves a largely improved water quality. Furthermore, it is shown that a small photovoltaic system can provide nearly all the energy required by such energy efficient pool system. This PV powered pool filtration system achieves a discounted payback period (DPP) of 5.4 years in comparison to the grid supplied pool filtration system (the Business as Usual (BAU) scenario).

*Keywords: low-speed pumping; pool chlorinator; pool cleaner; high-efficiency pool filtration.*

### Introduction

With the rapid growth of residential energy consumption and peak electricity demand, it is important to investigate the energy saving potential in households and so achieve higher energy efficiency. Studies have shown that households with a swimming pool have higher energy demand than households with no pools [1, 2]. The savings in pump energy used for solar pool heating was previously investigated by the authors and the results showed that operating the system at a lower flow rate reduced the pumping energy by 60%, without materially affecting the pool thermal performance [3]. This paper will investigate how to improve the energy efficiency of the pool filtration system by evaluating the performance of the whole system. Such system could achieve significant savings in energy and cost, which therefore enables its energy load to be supplied by a typical photovoltaic system.

### Background

Presently, there are approximately 1.1 million residential pools in Australia [4] and the total annual electricity demand is estimated be 2100 GWh per year [5]. This corresponds to approximately 2 million tonnes of carbon emissions per year [6]. Operating the pool filtration system under low flow conditions have been recognized as an energy efficiency retrofit by the industry and many swimming pool have adopted this measure [7]. Further, numerous studies have investigated the operation of pool filtration under low pump speed [8-11] with reported savings of as much as 80%. In addition, the use of a small photovoltaic system to power the low-energy pumping system was examined by Sproul [9] and the system achieved a 14 year payback period.

Although it is clear that significant amounts of energy could be saved by operating the pool filtration system under low flow conditions, the impacts on other system components such as the salt water chlorinators and the pool cleaners have not been widely reported. In addition to this, the associated effects on pool water quality yet have not been quantitatively examined. According to a recent report prepared for the Department of the Environment and Energy (DEE) of the Commonwealth of Australia, the most common type of Australian pool

is a salt water pool (60%) which relies on a chlorinator for sanitation [12]. The electrolysis process in the salt water chlorinator has been studied by Khouzam [13]; this process produces two gases, hydrogen gas and chlorine gas. The hydrogen gas is not soluble in water and therefore gets carried out of the chlorinator by the water flow, into the pool, and eventually into the environment. On the other hand, the chlorine gas, which is highly soluble in water, reacts with water to produce the hypochlorous acid (HOCl). The hypochlorous acid is known as free chlorine, which is an effective disinfectant in the pool. As in most cases, the same pump is used to both filter and chlorinate the water. One possible problem of operating the standard salt water chlorinators at low flow rate is that as the water flow reduces, the hydrogen gas produced accumulates in the chlorinator instead of being flushed out into the pool. Typically, chlorinators are designed to detect this dangerous situation and will switch off the chlorinator and the pump. Hence under these conditions, the pool sanitation deteriorates.

Additionally, a pressure pool cleaner powered by the filtration pump is also susceptible to low water flow operation, as the flow through the cleaners is shared with the pool skimmers or returns. Thus, to fulfill the cleaning task, the pump needs to run at a high speed for a certain period of time, which limits the extent to which the pool filtration can be completed at low flow rate using high-efficiency pumps.

Thus, it is the aim of this study to estimate the energy savings of the pool filtration system by taking the whole system into consideration. In particular, the low flow operation of the salt water chlorinator and the pressure pool cleaner are investigated to examine potential efficiency gains. To the authors' knowledge, there is no information available regarding the minimum operating flow rate of the chlorinator as well as its energy usage. Furthermore, energy efficient operating scenarios are proposed and the feasibility of utilising a PV system is analyzed.

**Experimental system**

Experiments were carried out on an existing domestic pool filtration system in Sydney Australia (Figure 1). The system has an eight-star variable speed water pump (Viron eVo P280), a controller, a salt water chlorinator (Hurlcon VX11T), an oversized cartridge filter (Viron CL400), and a pressure pool cleaner (Polaris 360) operated by the filtration pump. During the experiment key system parameters were monitored, which included the electrical power of the pump and chlorinator; water flow rates through the pump and the pressure pool cleaner; the pressure drop across the pump and the filter. A manually adjustable 3-way valve is located at the discharge of the chlorinator, which can change the proportion of water flow into the cleaner.

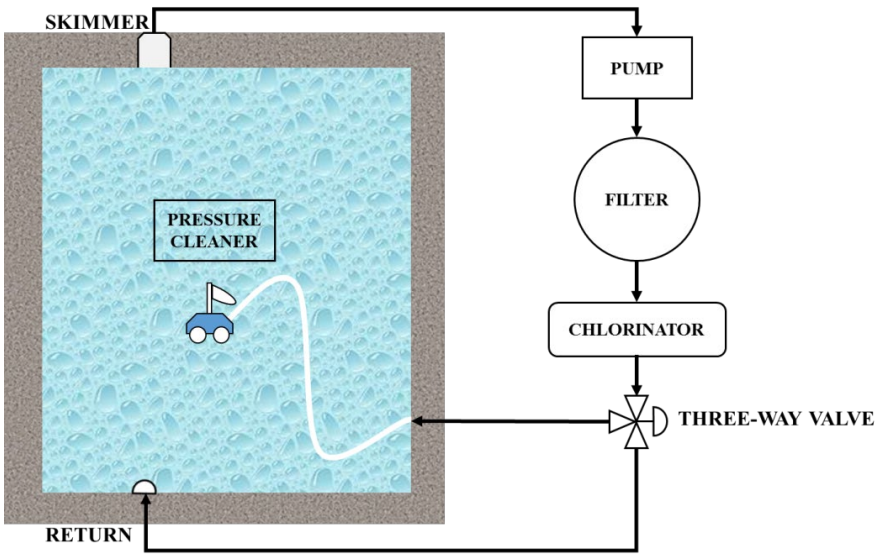


**Figure 1: Pool filtration system layout.**

**The controller coupled to the pump was used to set the operating schedule as well as the pump speed so that the system performance could be investigated under multiple operating scenarios, with different pump speeds and running times. The details of the operating scenarios are presented in**

Table 2. A robotic cleaner [14] was also retrofitted to replace the existing pressure cleaner in order to evaluate further energy saving opportunities.

Under each operating scenario, the water quality and cleaning effectiveness were examined qualitatively and quantitatively according to the requirements as per the Australian Standard AS3633 [15] and NSW Government [16] (Table 1). Based on the measured water quality, the chlorinator setting was adjusted manually using the controller until an acceptable water condition was obtained. Notice that as the pool water quality is affected by pool chemical levels as well as ambient factors including solar irradiance, the location of the pool, and its surroundings [13], the scenarios were varied out during the summer period to minimize variations due to the ambient weather conditions. Specifically, each scenario was carried out for 5 consecutive days with similar weather conditions (sunny and warm) and the daily water quality check was performed at 9 am.

**Table 1: Recommended pool water chemical concentrations [15, 16].**

| Parameters | Recommended range | |
|---|---|---|
| Free chlorine (ppm[1]) | Pool temperature < 26°C | > 2 |
| | Pool temperature ≥ 26°C | > 3 |
| pH | 7 – 7.8 (Optimum: 7.2 – 7.6) | |
| Total alkalinity (ppm) | 60 – 200 | |
| Isocyanuric acid (ppm) | 30 – 50 | |
| Calcium hardness (ppm) | 0 – 500 | |
| Total dissolved solids (ppm) | 1000 – 2000 | |
| Turbidity | 0.5 (NTU[2]) | |

**Operating the whole pool filtration system at low flow**

In order to assess the energy savings of running the variable speed pump at low speed, the comparison was made to the standard single speed pump investigated by Cunio and Sproul [10]. The Hurlcon 1500 W single speed pump was assumed to operate the same pool filtration system. The system operating point was obtained by overlaying the pump working curve with the measured system curve of the existing filtration system. The operating point was approximately 4.3 litre $s^{-1}$ at a head of 18.5 m. For such a single speed pump to fully turnover the pool once every day as required by the Australian Standard AS3633 [15], the daily pump energy is 3.6 kWh/day. This is comparable to the data reported by DEE [4], which stated that "*Australian households with a pool use on average 1352 kWh per year (3.7 kWh/day) powering pool pumps used for filtration.*".

Figure 2 shows the daily required pump running time calculated based on one pool turnover and the measured pump efficiency (pump efficiency was calculated as the ratio of measured hydraulic and electrical power). Also shown is the daily pump energy savings in comparison to the single speed filtration by operating the variable

[1] Parts per million. One ppm is equivalent to 1 milligram of something per litre of water (mg/l).
[2] Nephelometric Turbidity Units.

speed pump over its flow rate range. Note that the daily energy consumption of the variable speed filtration was calculated based on the measured power usage and the required running time at each flow rate. As can be seen, lowering the flow rate leads to a significant increase in the daily running time while the pump efficiency decreases drastically. However, even at the minimum flow rate, one pool turnover can still be accomplished within 24 hours.

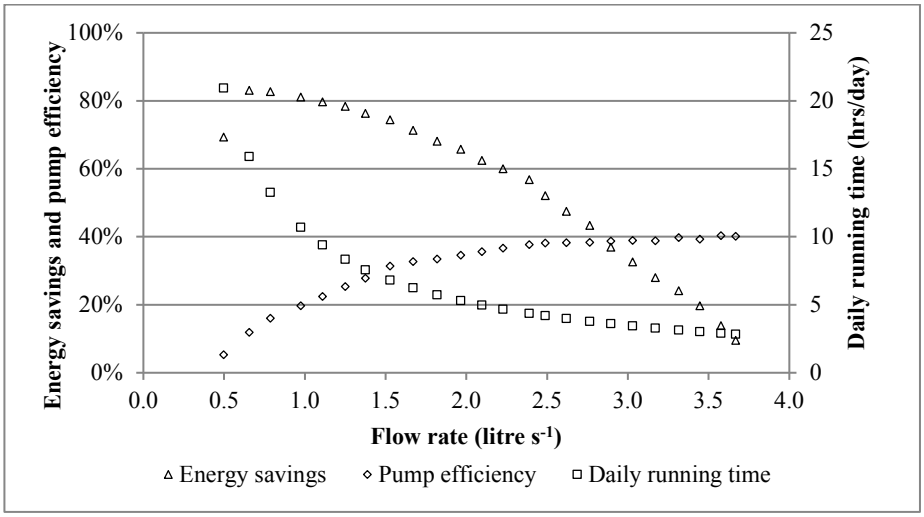


**Figure 2：Pump energy savings in comparison to the BAU case, daily running time and measured pump efficiency.**

Notice that even if the pump efficiency reduces by half, by operating the variable speed pump at a flow rate between 0.7 litre $s^{-1}$ to 1 litre $s^{-1}$, pump energy savings of over 80% can still be obtained. This amount of pump energy savings matches the finding reported by Sproul [9] and Cunio and Sproul [10]. However, the 80% energy savings were only contributed by the pool filtration pump, it is essential to adopt the whole system approach by taking other main system components into consideration, e.g. the pool chlorinator and the cleaner as shown in Figure 1.

Figure 3 shows the pressure drop across various system components. It can be seen that more than half of the total system pressure drop is due to the pipe and fittings. These include components that cause large pressure drop like the pool “eyeballs” (water inlet fittings), bends and tee pieces, and the three-way valve. It is also interesting to see that for flow rates below 1.7 litre $s^{-1}$ (pump speed of less than or equal to the default low speed), the pressure drop across the oversized cartridge filter is very small and therefore can be neglected. This confirms that oversizing the pool filter could reduce the overall pressure loss and achieve a better energy efficiency [17]. In addition, the existing pressure pool cleaner accounts for noticeable pressure loss, which is about one-third of the total system pressure. In comparison to the filtration system without the pressure pool cleaner, this reduces the flow rate under a specific pump speed and leads to a longer daily filtration period to change over the same amount of water. Though the pump uses lower power, the daily energy is more.

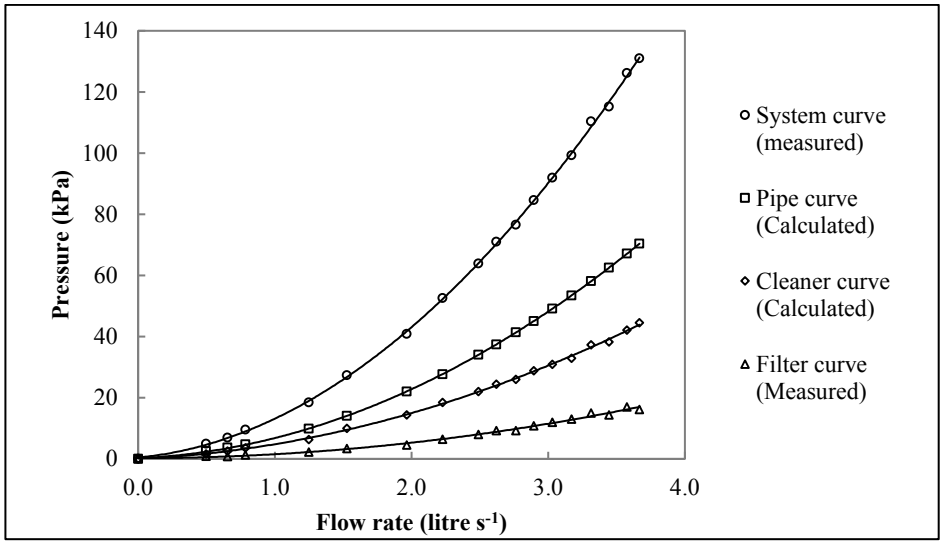


**Figure 3: Pressure drop across the pool filtration system components.**

**By operating the pool filtration system under various scenarios, the energy savings achieved at low flow conditions can be examined along with the associated effects on key system components.**

Table 2 shows the experimental results obtained by operating the whole pool filtration system under 7 scenarios. Also shown is the chlorinator setting for maintaining an acceptable pool water quality as per the Australian Standard AS3633 [15] for all scenarios. The Business as Usual (BAU) scenario is also presented, in which the variable speed pump was running at the highest speed and the chlorinator was at the highest setting. Notice that for scenario G, the pressure pool cleaner was disconnected and a robotic pool cleaner was used. Under this scenario, all flow was diverted through the pool returns by adjusting the three-way valve.

**Table 2: Experimental results of the whole pool filtration system operating under different scenarios.**

| Scenarios | A | B | C | D | E | F (BAU) | G |
|---|---|---|---|---|---|---|---|
| **Pump speed (RPM)** | 900 | 950 | 1150 | 1450 | 2075 | 2850 | 750 |
| **Cleaner type** | Pressure cleaner | | | | | | Robotic cleaner |
| **Filtration time (hrs/day)** | 14 (11 for one turnover) | 10 | 8 | 6 | 4 | 4 (2.8 for one turnover) | 10 |
| **Schedule** | 5am – 7pm | 7am – 5pm | 8am – 4pm | 9am – 3pm | 10am – 2pm | 10am – 2pm | 7am – 5pm Robotic cleaner (11 am – 12 pm) |
| **Flow rate (litre $s^{-1}$)** | 0.97 | 1.03 | 1.30 | 1.73 | 2.58 | 3.67 | 1.07 |
| **Chlorinator working?** | N | Y | | | | | |
| **Chlorinator setting (out of 8)** | N/A | 3 | 4 | 5 | 8 | 8 | 3 |

| | | | | | | | |
|---|---|---|---|---|---|---|---|
| **Proportion of flow through pool returns** | 0% | 0% | 0% | 24% | 50% | 65% | 100% |
| **Water chemistry** | Poor | Good | | | | | |
| **Water turbidity** | 3.2 | 0.82 | 0.45 | 0.41 | 0.43 | 0.4 | 0.24 |
| **Skimmer effectiveness and water clarity** | Poor | | | Ok for small and lightly polluted pools. | Good | | Perfect |
| **Manual clean?** | Y | | | | | | N |
| **Pool filtration system load (pump + chlorinator) (kW)** | | | | 0.29 | 0.62 | 1.36 | 0.12 (before 11 am and after 13 pm) 0.19 (11 am to 13 pm) |
| **Daily energy usage (kWh/day)** | | | | 1.8 | 2.6 | 5.5 | 1.5 |

The pool chlorinator stopped working when the flow rate dropped below 1 litre $s^{-1}$ due to insufficient flow and hydrogen accumulation. Hence under scenario A (flow rate of 0.97 litre $s^{-1}$), the pool water condition was heavily compromised – an unbalanced water chemical level and a turbidity of 3.2 NTU that was more than 6 times the recommended value of 0.5 shown in Table 1. This implies that 80% of savings of pump energy is actually not practical at a flow rate between 0.7 litre $s^{-1}$ to 1 litre $s^{-1}$. This is due to the hydrogen accumulation in the salt water chlorinator, which is shut down under such circumstances.

In terms of the pressure pool cleaner, the operating flow rate for achieving the proper wheel rotations (28 – 32 RPM) was approximately 1.3 litre $s^{-1}$ [18]. As seen from Table 2, under scenario A and B (flow rates of less than 1.3 litre $s^{-1}$), even if all flow was diverted into the pressure cleaner, its motion was still constricted and debris accumulated in the pool. By contrast, with proper adjustments of the existing three-way valve to meet the recommended flow range of the pressure cleaner, it was feasible to operate the pressure cleaner under scenario C to F. However for scenario C, the skimmer effects were heavily compromised since all flow was passed through the pressure cleaner. As a result, debris accumulated on the pool surface and this affected the pool clarity. The situation may get worse for heavily polluted areas.

From the whole of system performance perspective, it is more acceptable to operate the pool under scenario D (pump speed of 1450 RPM), where the three-way valve was adjusted to divert most of the flow (76%) through the pressure cleaner while still allowing some (24%) to allow the normal pool returns (“eyeballs”). This enabled the skimmer box and the pressure cleaner to be effective while running at the same time, therefore obtaining an appropriate pool condition. Notice that under scenario D, occasional manual cleaning was still needed to pick up the debris on the pool surface, especially during windy days.

After the robotic pool cleaner was retrofitted to replace the existing pressure cleaner, a significant improvement of pool cleanliness was observed (Figure 4). With the 4WD system, the robotic cleaner was able to climb on the pool steps and walls easily and perform cleaning without losing traction. In addition, since the water flow through the main pump was no longer needed to supply the pressure cleaner, all water flow was diverted via the normal pool returns and this allowed the skimmer box to operate more effectively. As a result, no manual work was required under this scenario to catch debris on pool surface nor to sweep the steps.

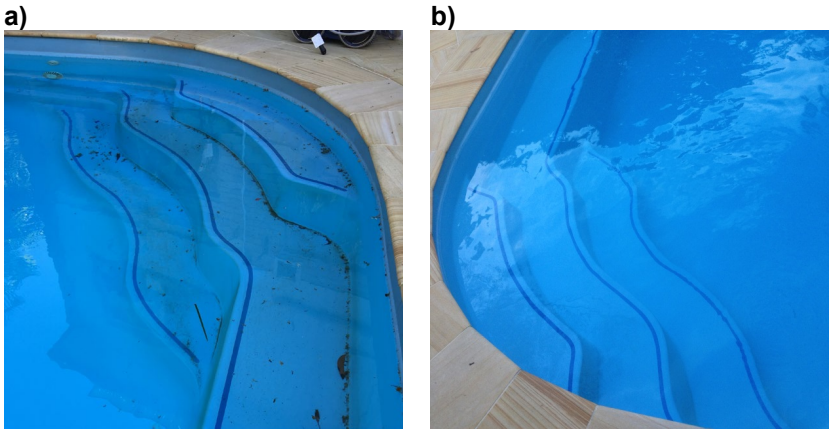


**Figure 4: Conditions of pool steps when the filtration system was operating under a) BAU scenario with a pressure cleaner, b) scenario G with a robotic cleaner (both with no manual cleaning) after a 24-hour period.**

Apart from the improved water clarity, it was also encouraging to see that the robotic cleaner was highly energy efficient and additional energy savings were obtained. Figure 5 shows the measured daily energy usage of the whole system operating under different scenarios. Notice that under these scenarios, all the system components were experimentally examined to work appropriately and the water quality was checked as acceptable.

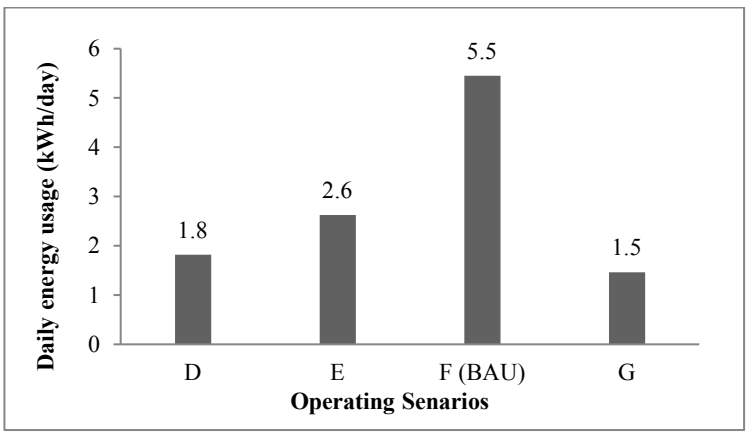


**Figure 5: Measured daily energy usage of the whole pool filtration system operating under various scenarios.**

For all scenarios with the pressure pool cleaner in use, the whole filtration system operating under scenario D consumed the least daily energy of 1.8 kWh/day. With a robotic cleaner in use (scenario G), the daily energy usage of the whole system was reduced to around 1.5 kWh/day. This is less than 30% of the BAU scenario (energy use of 5.5 kWh/day).

Assuming the pool filtration system is running year-round to maintain the pool conditions, the simple payback period of the whole system under the proposed energy efficient scenarios was calculated. Considering a variable speed pump (AU$1,500 including installation) as a retrofit option to the existing pool filtration system, operating the whole system at the minimum flow as required by the pressure cleaner (scenario D) has a simple payback period of approximately 3.4 years based on the electricity price of 0.323 AU$/kWh [19]. This is less

than the average pool pump lifetime of approximately 7 years [4], making it an ideal energy saving option for pool owners. For the energy efficient scenario G where a robotic cleaner is retrofitted, it takes around 6.5 years to pay back the total capital cost of the variable speed pump and the robotic pool cleaner. This is nearly double the payback of scenario D since the robotic pool cleaner costs about the same as the variable speed pump (AU$1,550). If low-cost robotic pool cleaners were developed, operating a variable speed pump at the lowest flow that suits the chlorinator (scenario G) would obtain a lower payback and therefore become a better solution considering its superior cleaning quality as demonstrated above.

**PV operated swimming pool filtration system**

Previous results showed that operating the pool filtration system under energy efficient scenarios (D & G) achieves significant energy savings and acceptable paybacks in comparison to the BAU scenario. It is also interesting to investigate the feasibility of running the whole system from a PV array. The simulation was carried out using NREL's System Advisor Model (SAM) [20] and the PV system was sized based on the BAU high-speed operation of the pool filtration system (scenario F in Table 2) in Sydney. The filtration system was assumed to operate year-round and the PV array was assumed to be connected to the grid. The key assumptions and parameters are shown in Table 3.

**Table 3: Assumptions and parameters of the PV system sized based on the BAU scenario (F).**

| | |
|---|---|
| **Nameplate capacity** | 2 kW |
| **Array orientation** | North |
| **Array tilt** | 34° |
| **PV module** | Suntech Power STP250-20/Wd |
| **Number of PV modules** | 8 |
| **Modules per string** | 8 |
| **Strings in parallel** | 1 |
| **Inverter** | Solar Power: YS-2000TL 277V |
| **Shading loss** | 0% |
| **Soiling loss** | 5% |
| **DC power loss** | 3% |
| **AC loss** | 1% |
| **Total module area** | 13 $m^2$ |

Figure 6 shows the power generated by the PV system at three different dates near to the: a) Spring (Autumn) Equinox, b) Summer Solstice, and c) Winter Solstice. Notice that two days around each date are presented to demonstrate the system performance under i) cloudy and ii) clear weather conditions. Also shown is the pool filtration system loads under BAU scenario, scenario D, and scenario G. The associated daily operating schedules and the energy loads are presented in Table 2..

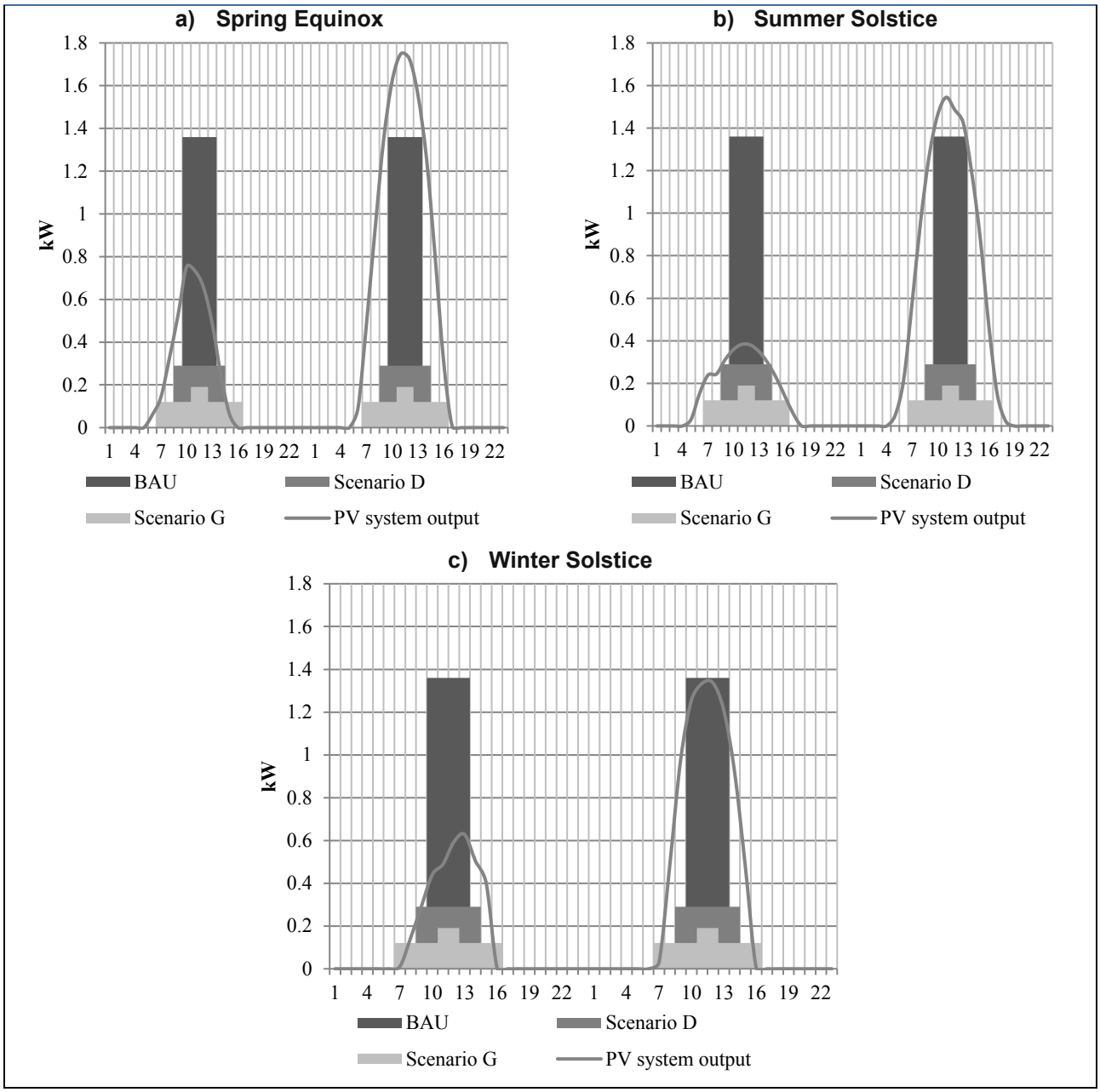


**Figure 6: PV system output and pool load under scenario D, G, and BAU for different sun positions in the southern hemisphere (left: cloudy day; right: clear day).**

It is clear from Figure 6 that on cloudy days, a majority of the pool load under the BAU scenario cannot be met by the PV system due to the significant decrease in the power generated. As seen from the SAM simulation results shown in Table 4, 423 kWh of electricity must be supplied annually by the grid under the BAU scenario and this leads to a PV fraction of only 45% (proportion of period where the pool filtration system load is completely covered by the PV system). By contrast, the same PV system is more likely to power the pool filtration system operating under energy efficient scenarios (D & G) even with bad weather. In both of these cases, only a small amount of electricity is sourced from the grid while the pool load can be fully supplied by the PV system for more than 90% of the total operating period (Table 4).

**Table 4: SAM simulation results of the pool filtration system operating under BAU scenario (both grid and PV powered), scenario D, and scenario G.**

| | BAU+Grid | BAU+PV | Scenario D (PV+Variable speed pump+Pressure cleaner) | Scenario G (PV+Variable speed pump+Robotic cleaner) |
|---|---|---|---|---|
| PV system output (kWh/yr) | 0 | 3017 | | |
| Excess PV output (kWh/yr) | 0 | 1,454 | 2,391 | 2,547 |
| Electricity from grid (kWh/yr) | 1,986 | 423 | 9 | 19 |
| Period with full load covered by PV (hrs/yr) | 0 | 651 | 2,083 | 3,399 |
| PV fraction | 0 | 45% | 95% | 93% |

Based on the results shown in Table 4, the net present values (NPV) and the discounted payback periods for the PV powered pool filtration systems were calculated relative to the BAU case: single speed pump, pressure cleaner, and grid-supplied system (BAU+Grid). The following parameters and assumptions were made for the calculations:

- Cost of system components:
  - Single speed pump: AU$ 775 [4].
  - Pressure pool cleaner: AU$ 720 (supplier).
  - Variable speed pump: AU$ 1,500 (supplier).
  - Robotic pool cleaner: AU$ 1,550 (supplier).
  - PV system: AU$ 5,868 [20].
- The lifetime of both pool cleaners are assumed the same as that of a typical pool pump, therefore all need to be replaced every 7 years [4].
- All the PV electricity generated is assumed to be self-consumed by the household.
- The discount rate is 5% [21].
- The grid electricity price is 0.323 AU$/kWh (including GST) [19]
- The grid electricity price is assumed to increase by 3% each year [22].
- The typical PV lifetime is 25 years [23].

**Table 5: Capital costs, net present values (NPV), and discounted payback periods (DPP) for PV powered pool filtration systems compared to BAU grid supplied system.**

| | **BAU+Grid** (Grid+Single speed pump+Pressure cleaner) | **BAU+PV** (PV+Single speed pump+Pressure cleaner) | **Scenario D** (PV+Variable speed pump+Pressure cleaner) | **Scenario G** (PV+Variable speed pump+Robotic cleaner) |
|---|---|---|---|---|
| Capital costs | AU$ 1,495 | AU$ 7,363 | AU$ 8,088 | AU$ 8,918 |
| NPV (relative to BAU+Grid) | AU$ 0 | AU$ 13,288 | AU$ 19,465 | AU$ 17,649 |
| DPP (years) | | 6.5 | 5.0 | 5.4 |

From Table 5, it can be seen that although the more efficient options have high upfront costs, the discounted payback periods for the two PV powered energy efficient systems (scenario D & G) are very attractive. In terms of scenario D, it has the highest NPV difference relative to the BAU grid supplied system and thus it is the most cost-effective solution. The whole system cost can be paid back in just 5 years, which is the shortest amongst three PV powered system considered. As for scenario G, due to the additional costs of the robotic pool cleaner and more electricity is purchased from the grid (Table 4), it needs around 5 months more for the whole system to pay back in comparison to scenario D. Nevertheless, it starts generating profits 1 year earlier than the BAU PV powered system (BAU+PV) and the discounted payback period is less than a quarter of the standard lifetime of a PV system. Considering that better pool quality and simpler pool maintenance can be achieved under scenario G, it is also an appropriate energy efficiency design of a residential pool filtration system.

## Conclusion

The study presents for the first time the results of a typical residential pool filtration system operating under various scenarios. The water flow rate was varied under different scenarios and the pool chlorinator was adjusted accordingly to deliver different chlorine production rates. For lower flow rates and longer running times, the rate of chorine production was reduced in comparison to the high flow rate operation. The pool water was also tested to ensure that the key water chemistry such as free chlorine and pH levels met the Australian Standard AS3633 [15] for all flow rates considered in this paper.

Experimental results revealed that over 80% of the pump energy could be saved by operating a variable speed pump at flow rates of less than 1 litre $s^{-1}$. However, at such flow rates, the salt water chlorinator and the pressure pool cleaner were identified not working properly and this led to unsatisfactory pool water conditions. For the pool filtration system considered in this study (with the pressure pool cleaner in use), it is more appropriate and energy efficient to operate the whole system at a flow rate of 1.7 litre $s^{-1}$ with a properly adjusted chlorinator setting (scenario D). The associated energy use is 1.8 kWh/day, which is approximately 33% of the energy use of the BAU scenario. In addition, the energy use reduces to 1.5 kWh/day with a robotic cleaner and the pool cleanliness is also substantially improved. For these energy efficient pool filtration systems, its load can be supplied by a small PV system. With no export of the PV electricity, it takes around 5 years and 5.4 years respectively for scenario D (pressure pool cleaner in use) and scenario G (robotic cleaner in use) to payback the initial investment (both refer to the discounted payback period with the replacement of pool system components taken into consideration). These discounted payback periods are less than 25% of the PV system lifetime.

Approximately 70% of the swimming pools in Australia are operated by single speed pumps [4]. If all of these pools were retrofitted to the energy efficient scenarios considered in this study, total energy savings of more than 1000 GWh and carbon reductions of nearly 1 million tonnes could be obtained annually [6]. Further, if all the low energy pool filtration systems were powered by PV systems where possible, total peak demand reductions of approximately 1 GW could be realized in Australia.

Except during periods of experimentation, the pool under study was operated under low flow conditions for approximately two swimming seasons. During this time water quality tests were undertaken, and readings were always in the acceptable range to maintain healthy swimming conditions as per the Australian Standard AS3633 [15]. In all circumstances, the filtration flow rates and pump run times were set so that the full volume of pool water was filtered once per day, as required by the Australian Standard AS3633 [15]. We would propose that provided this methodology was adhered to and that pool chemistry levels were maintained, the findings of this study should be generally applicable to different pool sizes, climates, and pool usage. However further studies of different pools would be useful to further verify the approach used in this paper.

**Acknowledgements**

This research is funded by the CRC for Low Carbon Living Ltd supported by the Cooperative Research Centre program, an Australian Government initiative. One of the authors (JZ) acknowledges scholarship funding provided by the Cooperative Research Centre for Low Carbon Living Ltd, as well as a scholarship from the Research Training Program of the Australian Government.

**References**

[1] A. Elnakat, J.D. Gomez, J. Roberts, M. Wright, Big data analysis of swimming pools' impact on household electric intensity in San Antonio, Texas, International Journal of Big Data Intelligence 2 (2015) 250-261.

[2] H. Fan, I.F. MacGill, A.B. Sproul, Statistical analysis of driving factors of residential energy demand in the greater Sydney region, Australia, Energy and Buildings 105 (2015) 9-25.

[3] J. Zhao, J.I. Bilbao, E.D. Spooner, A.B. Sproul, Experimental study of a solar pool heating system under lower flow and low pump speed conditions, Renewable Energy 119 (2018) 320-335.

[4] DEE, Consultation Regulation Impact Statement - Swimming Pool Pumps, Department of the Environment and Energy, Commonwealth of Australia, 2016.

[5] EES, Energy use in the Australian residential sector 1986-2020, Energy Efficient Strategies Pty Ltd (EES). Department of the Environment, Water, Heritage and the Arts, Commonwealth of Australia, 2008.

[6] DEE, National Greenhouse Accounts Factors, Department of the Environment and Energy, Commonwealth of Australia, 2018.

[7] DOE, Installing and Operating an Efficient Swimming Pool Pump. https://www.energy.gov/energysaver/installing-and-operating-efficient-swimming-pool-pump, 2018 (accessed 2018 April 29th).

[8] D. Springer, F. Rohe, Field Studies of Two-Speed and PV-Powered Pumps and Advanced Controls for Swimming Pools, ACEEE Summer Study on Energy Efficiency in Buildings “Profiting from Energy Efficiency” (1996)

[9] A.B. Sproul. Design of PV powered, high efficiency pool pump systems. in ANZSES solar energy conference. 2005.

[10] L.N. Cunio, A.B. Sproul. Optimising energy use in a domestic pool system. in 3rd International Solar Energy Society Conference 2008 (ISES 2008), 46th Australian New Zealand Solar Energy Society Conference. 2008.

[11] Z. Hameiri, E.D. Spooner, A.B. Sproul, High efficiency pool filtering systems utilising variable frequency drives, Renewable Energy 34 (2009) 450-455.

[12] Woolcott Research and Engagement, Pool Pumps: An Investigation of Swimming Pool Pumps in Australian and New Zealand, A research report prepared for the Department of the Environment and Energy, Commonwealth of Australia, 2016.

[13] K.Y. Khouzam. Electrolysis of salt water for chlorine production by photovoltaic power. in Power and Energy Society General Meeting-Conversion and Delivery of Electrical Energy in the 21st Century, 2008 IEEE. 2008. IEEE.

[14] Zodiac, Zodiac VX50 4WD Robotic Pool Cleaner. https://www.zodiac.com.au/vx50-4wd, 2017 (accessed 2017 March 3rd).

[15] Standards Australia, AS 3633-1989 - Private Swimming Pools - Water Quality, 1989.

[16] NSW Government, Swimming Pool Chemistry Testing Frequency. http://www.health.nsw.gov.au/environment/factsheets/Pages/swimming-pool-chemistry.aspx, 2013 (accessed 2017 September 8th).

[17] NRDC, Appliance Efficiency Pre-Rulemaking on Appliance Efficiency Regulations: Docket Number 12-AAER-2F - Residential Pool Pumps and Motors, Natural Resources Defense Council, 2013.

[18] Polaris, Polaris 360 Owner's Manual. http://www.polarispool.com.au/pressure/polaris-360, 2017 (accessed 2017 May 22nd).

[19] Energy Australia, Ausgrid zone: Basic Home (Standing Offer Tariff) - Peak Only. Energy Price Fact Sheet NSW Residential (Electricity). https://secure.energyaustralia.com.au/EnergyPriceFactSheets/PricingFactSheets.aspx, 2018 (accessed 2018 February 10th ).

[20] NREL, System Advisor Model, National Renewable Energy Laboratory, U.S. Department of Energy,

2017.
[21] E. Drury, P. Denholm, R. Margolis, Impact of Different Economic Performance Metrics on the Perceived Value of Solar Photovoltaics, National Renewable Energy Laboratory (NREL), Golden, CO., 2011.
[22] S. Kai, Energy prices—the story behind rising costs. http://www.aph.gov.au/About_Parliament/Parliamentary_Departments/Parliamentary_Library/pubs/BriefingBook44p/EnergyPrices, 2017 (accessed 2017 September 28th).
[23] NREL, Useful Life, Energy Technology Cost and Performance Data for Distributed Generation. http://www.nrel.gov/analysis/tech_footprint.html, 2017 (accessed 2017 June 22nd).

# Appendix 2

**Experimental study of a solar pool heating system under lower flow and low pump speed conditions**

**Jianzhou Zhao[1], Jose I. Bilbao[1], Edward D. Spooner[2] and Alistair B. Sproul[1]**

[1] *School of Photovoltaic and Renewable Energy Engineering, UNSW, Sydney (Australia)*

[2] *School of Electrical Engineering and Telecommunications, UNSW, Sydney (Australia)*

## Abstract

Operation of an unglazed, open-loop, solar collector for residential pool heating was investigated experimentally under various flow conditions. The objective of this work was to examine if solar pool collectors can be operated at lower flow conditions to minimise the pump energy while still providing sufficient thermal energy output to heat the pool. The system consists of a 20.5 $m^2$ plastic tube, solar collector and a 36 $m^2$ in-ground open-air pool. Key parameters were monitored over 38 days during summer and used to validate a steady state model. The model achieved a good fit against the measured data and was used to simulate the system performance under various scenarios. Operating the system at low pump speed with a mass flow rate per unit collector area ($\dot{m}/A_C$) of 0.016 kg $s^{-1}$ $m^{-2}$ was found to be optimal and achieved approximately 60% pump energy savings. The coefficient of performance was increased by 2.5 times without compromising the thermal performance of the system in comparison to the high pump speed operation (the Business as Usual (BAU) case). The optimal $\dot{m}/A_C$ is approximately 20% of the *BAU* value (0.076 kg $s^{-1}$ $m^{-2}$) and below the lower limit specified by International and Australian Standards (0.03 kg $s^{-1}$ $m^{-2}$). Assuming all such systems in Australia were operated at a lower flow rate and with a low energy pump, annually around 180 GWh of electricity could be saved and 150 kilotonnes of carbon dioxide emissions could be avoided.

*Keywords: Solar collector; swimming pool; lower flow rate; low pump speed, high efficiency pumping*

## 1. Introduction

Approximately 15% of Australian households have a swimming pool and the associated pumping system is usually the largest energy user in these households [1]. For typical Australian households with pools, a pool pump consumes over 1500 kWh per year and comprises around 18% of the total electricity consumption [2]. Additionally, numerous studies have shown that households with a swimming pool have higher energy demand than households without a pool. For example, Elnakat et al. [3] reported households with pools in the U.S. use 40% more energy, while Fan et al. [4] also found that households with a pool have significantly higher daily electricity demand than those without one in the greater Sydney region, Australia. As a result, the operation of swimming pools increases a household's electricity costs significantly, and it also has significant impacts on the peak electricity demand and the environment. Seebacher [5] addressed the contributions of swimming pools to peak demand, and found that on average each pool added an additional load of around 1.2 kW. Further, Ergon Energy, one of the major electricity suppliers in Australia, also reported an average load of 1.1 kW is due to a swimming pool that is normally operated during residential peak demand periods [6]. From the environmental perspective, the projected pool energy usage in 2017 will contribute approximately 1.9 Mt per year of greenhouse gas emissions [7] and this corresponds to approximately 0.35% of Australian's total annual greenhouse gas emissions [8].

Besides pool filtration, pool heating is another major driver of the energy demand, which accounts for around 27% of the total energy usage of a pool [9]. Approximately one third of Australian pools are heated and whilst some gas heaters and heat pumps are utilised, about 90% of heated, residential pools in Australia are heated using solar collectors [10, 11]. In comparison to a heat pump or gas heating, solar pool heating has significantly lower operating costs and carbon emissions, as presented in Table 1 [12]. The data shows that solar pool heating uses only about 14% of the energy of a heat pump, and 3% of the energy of a gas heater, with similar savings on greenhouse gas emissions.

**Table 1 Energy usage and GHG emissions of different pool heating types [12].**

| | Solar pool heating | Heat pump pool heating | Gas pool heating |
|---|---|---|---|
| Estimated daily energy usage | 6 kWh | 43 kWh | 218 kWh |
| Greenhouse Gas Emissions per week | 45 kg | 290 kg | 360 kg |

Other active pool heating systems utilizing other renewable energy sources (RES) can also be found in the literature. Katsaprakakis [13] compared various passive and active pool heating systems in Southern Europe, which included the pool enclosure, insulating covers, biomass heaters coupled with solar collectors, and geothermal heat exchangers combined with geothermal heat pumps in Southern European locations [13]. The results show that the use of pool insulation covers led to considerable savings in pool heating loads, and the remaining energy demand could be met by a RES based system with an investment payback of less than 5 years. More complex pool heating systems using heat recovery options were also investigated in various studies [14, 15]. Such systems use the waste heat produced by cooling devices to heat the pools (for example, one system used waste heat from an ice rink to heat a nearby swimming pool). However, such studies are outside the scope of the present work, which is focused on residential pool heating and in particular, solar pool heating systems.

For pool pump systems associated with filtration and cleaning of pool water, considerable energy savings have been achieved through the use of multi-speed or variable speed pumps. By operating pool filtration pumps at 25 – 35% of a typical flow rate for a pool, pump running times are increased however, energy savings of the order of 60 – 80% have been achieved [16-18]. To date however, there have been very few reports of this approach being adopted for solar pool heating systems. Hence, the objective of this work is to examine if solar pool collectors can be operated at lower flow conditions to minimise the pump energy while still providing sufficient thermal energy output to heat the pool.

## 2. Literature review

In the past few decades, there has been considerable research into the direct use of solar thermal collectors for swimming pool heating [19-29]. As the thermal performance of the solar collector depends largely on the water flow rate [30], a wide range of mass flow rates per unit collector area ($\dot{m}/A_C$), have been reported in the literature for solar pool heating collectors.

An early technical report by Czarnecki [19] addressed the basic design considerations of solar pool heating systems. It recommended a minimum value for $\dot{m}/A_C$ of 0.02 kg $s^{-1}$ $m^{-2}$ in order to ensure a low operating temperature of the solar collectors. A similar value for the mass flow rate per unit collector area of 0.018 kg $s^{-1}$ $m^{-2}$ was adopted by Sodha and Kumar [23] when investigating the solar heating of open swimming pools in India. They pointed out that the swimming season could be largely extended when a plastic solar collector was used (area of 75% of the pool area) along with a pool cover. Cusido and Puigdomenech [21] designed and built a high efficiency, low cost solar collector used for pool heating in Mediterranean climate and a flow rate of 1.4 kg s-1 was chosen to avoid any turbulent flow in the pool. This translates to a much higher $\dot{m}/A_C$ of around 0.13 kg $s^{-1}$ $m^{-2}$ given that the collector area was only 11 m2. Molineaux and Lachal [26] carried out an experimental analysis of five unglazed, plastic solar collectors used for heating outdoor swimming pools in Switzerland. Their results indicated that the collector efficiency was not affected significantly by large heat losses due to the low temperatures involved. As such, the unglazed solar collectors were considered as suitable for low temperature applications like swimming pool heating. The experimental data was obtained by operating the solar collector under five different $\dot{m}/A_C$ values, which ranged from 0.028 to 0.11 kg $s^{-1}$ $m^{-2}$. Dongellini and Falcioni [29], more recently, modelled the performance of three types of flat solar collector (unglazed, glazed and evacuated). The study highlighted that the unglazed and evacuated collectors were appropriate for swimming pool heating due to their high efficiency at low values of $\Delta T/G$ (temperature difference between pool water and ambient air over the solar irradiance), while the evacuated collector was more suitable for larger pools. In their simulations, the authors used a fixed value of $\dot{m}/A_C$ of 0.015 kg $s^{-1}$ $m^{-2}$. It is important to note that for all the literature cited, the values for $\dot{m}/A_C$ were simply chosen by the authors with no justifications provided.

In contrast, very few studies have addressed the issue of the optimal flow rate for solar pool collectors and very few have considered the pump energy required. Medved and Arkar [27] analysed an unglazed solar pool collector and the optimization of the flow rate was performed only based on maximizing the thermal efficiency of the collector without considering the energy consumed by the pump. The suggested flow rates ranged from 0.008 to 0.023 kg $s^{-1}$ $m^{-2}$ for steel

absorbers, and 0.014 to 0.027 kg $s^{-1}$ $m^{-2}$ for aluminium absorbers. Further their model was simply validated with a fixed wind speed due to the incomplete data during the short experimental period. Similarly, the required pump energy was also excluded by Baughn and Young [31], who conducted a computer based optimization of the flow rate for a typical solar domestic hot water (SDHW) system. They reported an extremely low optimal value for $\dot{m}/A_C$ of 0.005 kg $s^{-1}$ $m^{-2}$, which led to a very low pump power (<1 W). Therefore, the pump energy was deemed to be negligible if the pump was properly sized. This approach (ignoring the pump energy) however is not appropriate for a solar pool heating system, where the pump needs to move much larger volumes of water, provide sufficient pressure to overcome the total dynamic head of the system and importantly to ensure the vacuum relief valve remains closed [32, 33]. As water pumps are an essential component in solar pool heating, some studies accounted for the associated energy when optimizing the flow rate. Kovarik and Lesse [34] and Winn and Winn [35] discussed the optimal control of flow rate to achieve the maximum difference between the collected thermal energy and pump energy. A solar hot water system was examined and the optimal flow rate was reported as 0.027 kg $s^{-1}$ $m^{-2}$at peak solar irradiance [34].

Also there are numerous studies that have considered exergy for optimizing solar thermal system performance [36, 37]. However, maximising exergy is only an appropriate objective when the goal is to maximise the amount of useful work to be done by the system [38]. For solar pool collectors and for many other solar thermal systems, the objective is to produce low grade heat, not work. Therefore, in these cases maximising exergy is not the correct objective, and it is more appropriate to maximize the COP in order to obtain the maximum thermal energy with minimum electrical energy input and cost [30, 39].

To the authors knowledge, only Cunio and Sproul [28] have evaluated the solar pool heating collector performance at lower flow rates and lower pump power in order to improve COP. Their experimental results showed that the solar collector's thermal efficiency was only reduced by approximately 15% when operating at lower flow rates, while the COP of the system increased substantially. More importantly, up to 80% of the pumping energy could be saved, and the decrease in the solar collector heat output due to the lower flow could be offset by increasing the collector area or extending the system-running time. However, the pumping system investigated was a single speed, high power pump (750 W) and its flow rate was adjusted using a throttle valve in order to investigate the thermal performance of the solar collector under lower flow rates. Furthermore, the pump power, pump energy savings, and COP were not measured experimentally, but instead were estimated based on the obtained performance system curve. Additionally, the sky temperature was not considered when modelling the system performance and the reported COP was calculated only for high solar irradiance conditions (approximately > 800 W $m^{-2}$).

In summary, a wide range of mass flow rates per unit collector area were found for solar pool collectors. For example, low values have been reported in the range of 0.015 – 0.03 kg $s^{-1}$ $m^{-2}$ [19, 23, 26-29] as well as higher values in the range of 0.11 – 0.13 kg $s^{-1}$ $m^{-2}$[19, 21, 26]. Further, the International standard ISO/TR 12596 [32] and the Australian Standard AS 3634 [33] specify the recommended value of $\dot{m}/A_C$ for unglazed solar pool collectors to be in the range of 0.03 – 0.04 kg $s^{-1}$ $m^{-2}$ and 0.03 – 0.08 kg $s^{-1}$ $m^{-2}$ respectively. However, very few studies have provided appropriate reasons as to why the flow rates were proposed. In addition, many different approaches have been reported that aim to maximise the performance of solar pool heating systems by optimizing the flow rate. In previous studies, some aimed to maximize only the thermal efficiency of the collector or the exergy of the system or the difference in thermal energy output and pump energy input. However, we propose that the correct approach is to maximise the COP of the solar pool heating system.

It is important that the COP be calculated in terms of an energy ratio:

$$COP = \frac{Q_u}{W_{pump}} \quad (1)$$

where $Q_u$ is the heat output of the solar pool collector (typical units of kWhth) and $W_{pump}$ is the electrical energy supplied to the pump (units of kWhe) over a defined period. It is important to note that the dominant operational cost for a solar pool heater is the electrical energy supplied to the pump. Hence by maximising the COP, this will minimize the pump energy and hence minimize the operational cost of the system, while still needing to ensure the system is capable of providing sufficient thermal output to heat the pool.

## 3. Methodology

This study utilises the COP (energy ratio) approach to determine the optimal flow rate for solar pool collector systems in order to minimise the electrical energy required for the pump while still providing sufficient thermal energy output to heat the pool. Previous work by Cunio and Sproul [28] explored the concept of using low speed pumps and lower flow rates to minimize pump energy and obtain higher COP than previously reported. This present paper builds on the work of Cunio and Sproul and presents for the first time experimental results obtained using a commercially available 3-speed pool pump (default speeds of 2000, 2410, and 2850 RPM) to operate a solar pool heating system under lower flow rate conditions. A brief overview of the methodology is presented below:

1) A theoretical model of the solar collector and open-air swimming pool was developed in TRNSYS.
2) A measurement system was designed and installed on an existing solar collector and pool located in Sydney, Australia.
3) Experimental data under various pump speeds and flow rates over a period of time was collected. The following parameters were measured:
    - Solar pump: pressure, power and energy.
    - Solar collector: flow rates, inlet and outlet water temperatures.
    - Weather parameters: solar irradiance, air temperature and wind velocity.
4) The TRNSYS model was validated against the experimental results.
5) The validated TRNSYS model was then utilised to determine the optimal flow rate under standard test conditions (irradiance 800 W $m^{-2}$, wind speed 3 m $s^{-1}$, ambient temperature 25°C) in order to achieve a 1°C temperature rise in the pool.
6) The whole system performance using the optimal flow rate over the summer period in the southern hemisphere (October to March) was investigated to determine the system performance.

More details of the methodology employed in this study will be presented in subsequent sections.

## 4. Theoretical model of the solar pool heating system

### 4.1 Unglazed solar collector model

The model developed for this study is a steady state unglazed solar collector based on the standard equations provided by Duffie and Beckman [30]. A thermal resistance approach reported by Bambrook and Sproul [40] was used to model the collector. The rate of the heat output from the unglazed solar collector is expressed as follows:

$$\dot{Q}_u = A_C F_R \left[\alpha_c G - \frac{T_{in} - T_a}{R_L}\right] \quad (2)$$

where $A_C$ is the solar collector surface area, FR is the collector heat removal factor, $\alpha_c$ is the collector solar absorption, $G$ is the solar irradiance in the collector plane, $T_{in}$ is the collector fluid inlet temperature, $T_a$ is the ambient air temperature near the solar collector and $R_L$ is the total thermal resistance from collector surface to the ambient as given by Duffie and Beckman [30]:

$$\frac{1}{R_L} = \frac{1}{R_{r,s_{eff}}} + \frac{1}{R_w} + \frac{1}{R_{r,r_{eff}}} \quad (3)$$

where $R_w$ is convective thermal resistance due to wind, and $R_{r,s_{eff}}$ and $R_{r,r_{eff}}$ represent the effective radiative thermal resistance from collector surface to the sky and to the roof respectively [38]. Since the roof has a varying profile and is non-uniformly shaded by the collector and surroundings, its average surface temperature is difficult to determine. Hence for simplicity, the roof temperature was initially assumed to be a constant 5 K less than the collector temperature, based on the estimation provided by Cunio and Sproul [28]. The sky temperature was also taken into consideration as it has a substantial impact on the thermal performance of unglazed solar collectors [41]. The sky temperature was calculated using the equations provided by Martin and Berdahl [42]. The convective thermal resistance due to wind above the collector ($R_w$)

is highly dependent on the individual experiment and collector characteristics and therefore varies across different studies [43-45]. Bilbao [46] has shown that the expression reported by McAdams [43] has been widely used and provides a good agreement between simulation results and experimental data for unglazed collectors. Therefore, the expression reported by McAdams [43] (Eqn. 4) was used as the theoretical expression for convective thermal resistance due to wind for the solar pool collector model.

$$R_w = \frac{1}{5.7 + 3.8V_{W_c}} \quad (4)$$

where $V_{W_c}$ is the wind velocity over the solar collector.

### 4.2 Open-air swimming pool model

The residential outdoor swimming pool under investigation has a total surface area of 36 m$^2$ and a volume of 37,500 litres. The pool water temperature was assumed as uniform due to the circulation of the filter pump and the presence of pool users [47]. The heat balance of an open-air swimming pool is given by:

$$V_{pool}\rho_w C_p \frac{dT_{pool}}{dt} = \dot{Q}_u + \dot{Q}_{sol} - \dot{Q}_{loss} \quad (5)$$

where $V_{pool}$ is the pool volume, $\rho_w$ is the pool water density, $C_p$ is the specific heat of water, $T_{pool}$ is the pool temperature, $\dot{Q}_u$ is the rate of heat output from the solar collector and $\dot{Q}_{loss}$ is the rate of heat loss from the pool. The term $\dot{Q}_{sol}$ is the rate of pool heat gain due to the absorption of solar irradiance, which in turn is given by:

$$\dot{Q}_{sol} = A_{pool}\alpha_p G(1 - f_{shade}) \quad (6)$$

where $A_{pool}$ is the pool surface area, $\alpha_p$ is the pool solar absorption, and $f_{shade}$ is the pool shading factor. The pool investigated in this study is a light-coloured pool and there are a range of pool solar absorption values reported in the literature for such pools. The International standard ISO/TR 12596 and the Australian Standard AS3634 both report a value of 0.85 [32, 33]. This value was also used by Hahne and Kübler [25], Lam and Chan [48], and Ruiz and Martínez [49] and good fits were obtained between modelled and experimental data. Therefore, a value of 0.85 was used for the pool solar absorption in this study. The pool shading factor ($f_{shade}$) represents the proportion of the pool shaded by surrounding objects. It was estimated by the model developed utilising SketchUp and further details are given in section 7.4.

The rate of pool heat loss ($\dot{Q}_{loss}$) (W) is a combination of the heat losses due to evaporation, radiation, and convection:

$$\dot{Q}_{loss} = \dot{Q}_{evap} + \dot{Q}_{rad} + \dot{Q}_{conv} \quad (7)$$

Other heat losses are the conduction heat loss due to the temperature difference between the pool internal surface and the ground and the heat loss introduced by makeup water. These losses are considered relatively small and are normally neglected in pool models [25, 49].

The rate of pool heat loss due to evaporation $\dot{Q}_{evap}$ is given by:

$$\dot{Q}_{evap} = A_{pool}h_{evap}(P_W - P_V) \quad (8)$$

where $P_W$ and $P_V$ are the saturation water vapour pressure at water temperature and the partial water vapour pressure in the air respectively, and $h_{evap}$ is the evaporative heat transfer coefficient of the pool and it has a strong dependence on the local wind conditions [25]. The evaporative heat transfer coefficient reported by Richter [50] was found to give the best agreement between the modelled and measured results for one of the pools investigated by Hahne and Kübler [25]. Ruiz and Martínez (2010) have also validated the same expression based on a household open-air pool. Therefore, the expression proposed by Richter [50] was used as the theoretical expression for the evaporative heat transfer coefficient of the pool in this study.

$$h_{evap} = 42.3 + 56.6V_{W_p}^{0.5} \quad (9)$$

where $V_{W_p}$ is the wind velocity over the pool. It can be calculated by multiplying the measured wind speed ($V_{W_c}$) with a factor of 0.15 for well-sheltered sites [33].

## 5. Experimental system

### 5.1 Experimental setup

The test pool system is located in a suburb of Sydney, New South Wales, Australia. It has a secondary water pump for solar heating purpose which pumps water via 40 mm pressure pipes into a solar pool collector. The unglazed solar collector under investigation is mounted on the roof of a residential home and the height from the pool surface to the highest point of the collector was measured as 5.5 m. The plastic strip solar collector (Fig. 1a) has 2 mats, each consisting of 160 black tubes connected in parallel. The Viron P280 3-speed water pump (Fig. 1b) can operate at high speed (2850 RPM) in order to provide sufficient pressure to overcome the initial static head during start-up. A vacuum relief valve (Fig. 1c) was installed at the highest point in the solar pool heating system, which is designed to avoid operating the collector with water below atmospheric pressure and allows water to drain out when the solar pump is switched off. A throttle valve (Fig. 1d) was installed on the pipeline where heated water flows back into the pool, which can be used to restrict the flow rate to keep the vacuum relief valve closed during operation. This will be discussed further below.

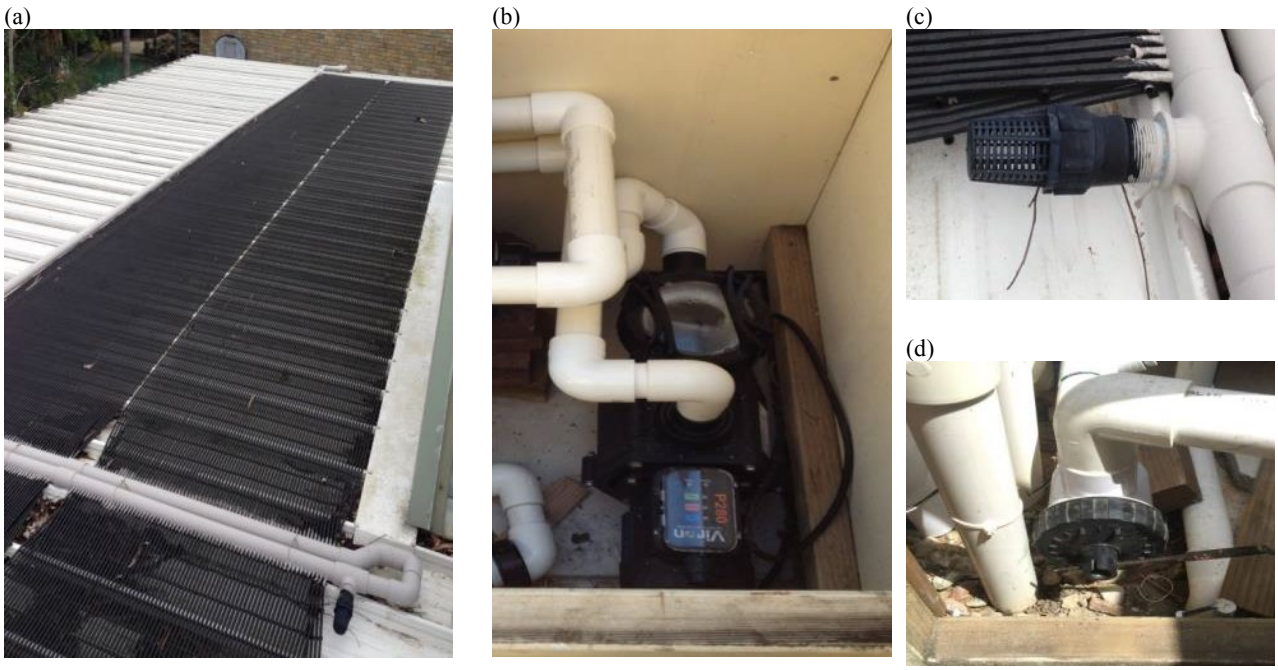


**Fig. 1. (a) unglazed solar collector, (b) Viron P280 3-speed water pump, (c) vacuum relief valve, (d) throttle valve.**

The experimental system layout is shown in Fig. 2 below. Two RTD water temperature sensors were mounted on the collector inlet and outlet, and a flow meter was installed at the pump outlet. A rooftop weather station was installed near the solar collector to measure the ambient weather data (temperature, wind speed and solar irradiance). The pump energy consumption was measured with a digital power meter. All the measurement data was collected by a data acquisition system with 1 second sampling rate. The collected data was then averaged over 10 minute intervals for further analysis. The data resolution of 10 minutes was three times the collector time constant of approximately 3.5 minutes, which was calculated based on the approach specified by International Standard ISO 9806 [51]. The experimental equipment details and the calculated uncertainty of the major system parameters (using the equations provided by Taylor [52]) are given in Table 2.

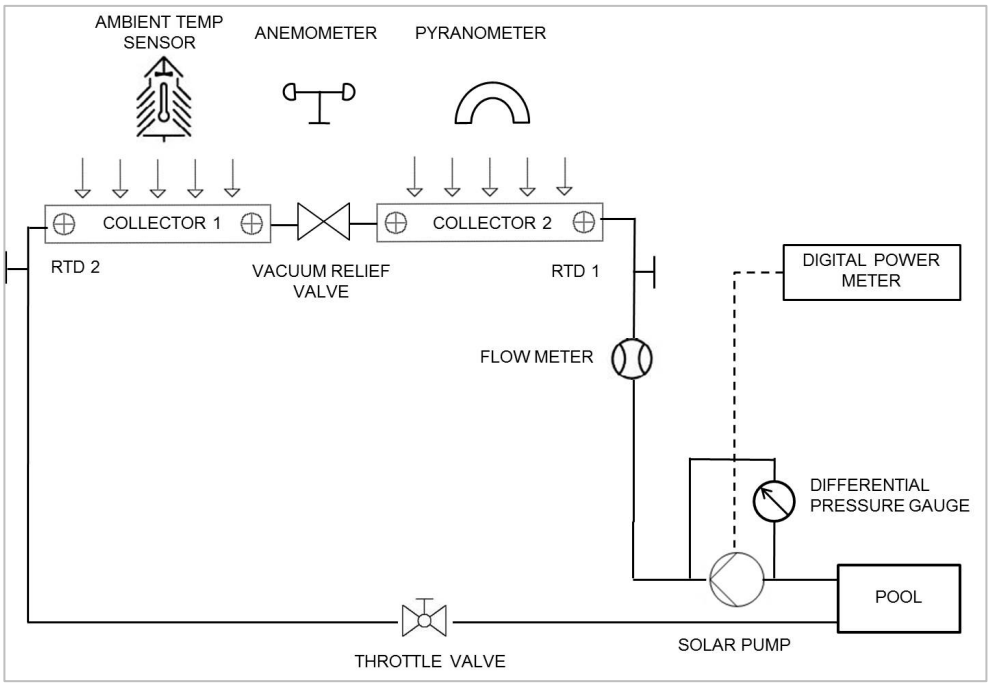


**Fig. 2. Experimental system layout.**

**Table 2 Experimental equipment and uncertainties and uncertainties of calculated parameters based on experimental data.**

| Equipment | Measurement | Uncertainty |
|---|---|---|
| Manu Rota Pulse Flow Sensor | Mass flow rate ($kgs^{-1}$) | ±2.5% |
| RTD Temperature Sensor PT100 | Inlet water temperature (Pool temperature) (°C) | ±0.03°C |
| RTD Temperature Sensor PT100 | Outlet water temperature (°C) | ±0.03°C |
| RTD Temperature Sensor PT100 | Air temperature (°C) | ±0.03°C |
| Intech 3 Cup Anemometer WS3-CL | Wind velocity ($ms^{-1}$) | ±2% |
| Saia Energy Meter AAD1 | Power and energy consumption (W and Wh) | ±1% |
| Kipp & Zonen Pyranometer CM5 | Solar irradiance ($Wm^{-2}$) | ±5% |
| Dwyer Diff. Pressure Transmitter Series 629 | Water pump pressure (psi) | ±0.5% |
| DataTaker DT80 Series 3 data logger | All input measurements | ±0.1% |

| Parameter | Uncertainty |
|---|---|
| Collector water temperature rise ($\Delta T$) | ±0.04°C |
| Electrical power supplied to the pump ($\dot{W}_{pump}$) | ±1% |
| Rate of heat output of the solar collector ($\dot{Q}_u$) | ±2.54% |
| Coefficient of Performance ($COP_r$) | ±2.73% |

## 5.2 The operation of the solar pool heating system

As previously mentioned, the pump is a substantial component in the system, which provides water circulation by generating sufficient pressure to overcome the total dynamic head and keep the vacuum relief valve closed. Once the whole system is primed, from the energy analysis of steady flows [38], the pressure developed by the pump is simply the pressure drop due to friction in the pipe, pipe fittings, and the solar collector for the whole system, which is given by:

$$\Delta P_{pump} = \Delta P_{loss} = \Delta P_{pool\_vac} + \Delta P_{vac\_pool} \quad (10)$$

where $\Delta P_{pump}$ is the pump pressure, $\Delta P_{loss}$ is the pressure drop for the whole system, $\Delta P_{pool\_vac}$ is the pressure loss from the pool skimmer box to the vacuum relief valve, and $\Delta P_{vac\_pool}$ is the pressure loss from the vacuum relief valve to the pool return.

Using a similar analysis as above [38], pressure inside the pipe near the vacuum relief valve at the highest point ($P_{vac}$) is given by:

$$P_{vac} = P_a + \Delta P_{vac\_pool} - \rho_w g H - \frac{1}{2}\rho_w V_{av}^2 \quad (11)$$

where $P_a$ is the atmospheric pressure, H is the height of the vacuum relief valve above the pool water level, and $V_{av}$ is the average velocity of the water in the pipe at the location of the vacuum valve.

For the vacuum relief valve to remain closed, $P_{vac}$ must be higher than $P_a$, that is:

$$P_{vac} - P_a = \Delta P_{vac\_pool} - \rho_w g H - \frac{1}{2}\rho_w V_{av}^2 > 0 \quad (12)$$

Therefore, the minimum pump pressure required to keep the vacuum relief valve closed can be calculated based on Eqns. 10 and 12, which is given by:

$$\Delta P_{pump} > \frac{1}{2}\rho_w V_{av}^2 + \Delta P_{pool\_vac} + \rho_w g H \quad (13)$$

Fig. 3 shows the measured pump pressure curves for the Viron P280 pump at the 3 default pumping speeds. They were obtained by measuring the pressure across the pump at various flow rates by adjusting the existing throttle valve (Fig. 1d). Also shown is the calculated pump pressure required to close the vacuum relief valve as per Eqn. 13.

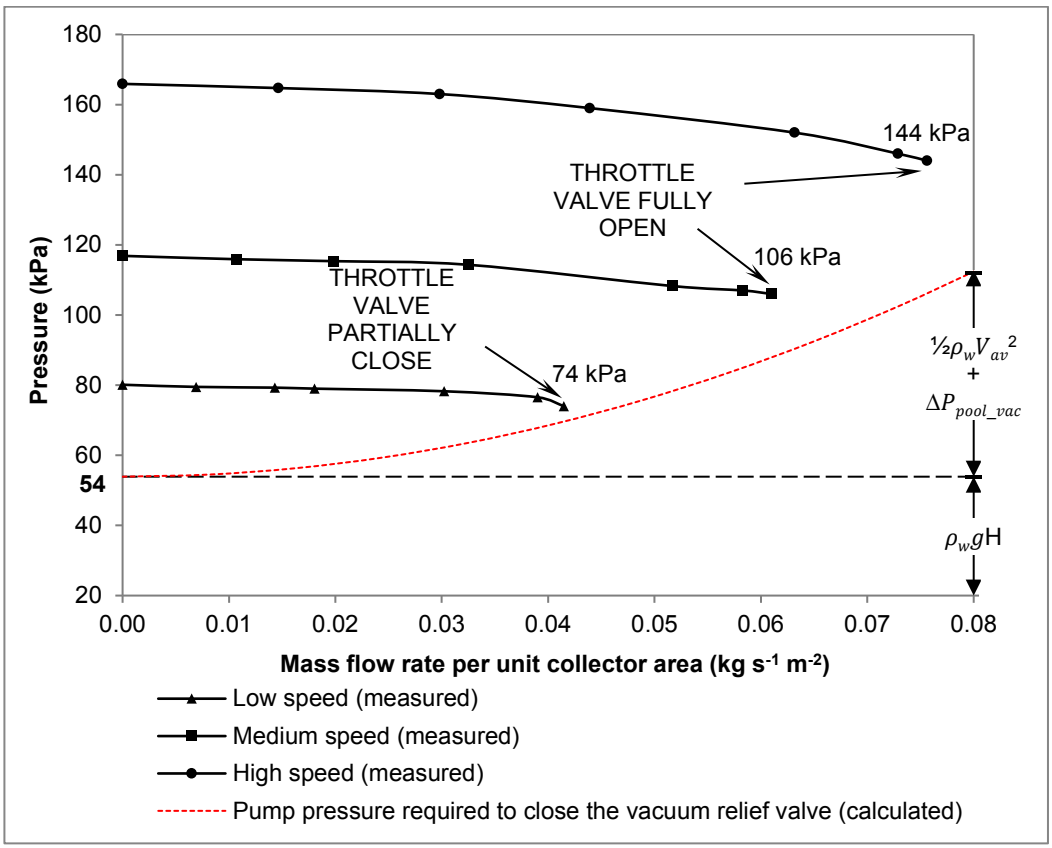


**Fig. 3 Experimentally measured AstralPool Viron P280 pump pressure at three speeds and calculated pump pressure for the vacuum relief valve to close.**

The height of the vacuum relief valve above the pool water level (H) was measured as 5.5 m, which corresponds to a static pressure ($\rho_w gH$) of 54 kPa. It is worth noticing that at a low pump speed (2000 RPM), the throttle valve has to be partially closed in order to generate sufficient pressure to close the vacuum relief valve (shown in Fig. 3). The minimum pump pressure measured for the lowest speed setting of the pump is 74 kPa, which is slightly higher than the required pump pressure calculated. This may possibly due to the spring load inside the vacuum relief valve which adds extra pressure. The throttle position that keeps the vacuum relief valve closed, with minimum pressure at the low speed of the pump, is designated as the minimum throttle position. If the throttle valve was opened further from this minimum throttle position, the vacuum relief valve would open and the system would lose its prime.

On the other hand, the throttle valve can be fully opened at medium and high speed without losing the water circulation of the whole system. At the high pump speed (2850 RPM), the minimum pump pressure with the throttle valve open is around 140 kPa and the corresponding flow rate is 0.076 kg $s^{-1}$ $m^{-2}$. For a typical single speed pump used in Australian solar pool heating systems (e.g. AstralPool E-series E230 pump [53]), the pump can generate approximately the same amount of pressure (total head of 14 meters) at the same flow rate. In addition, this highest flow rate measured at the high pump speed is within the recommended working flow rate for unglazed solar collectors (0.03 kg $s^{-1}$ $m^{-2}$ – 0.08 kg $s^{-1}$ $m^{-2}$) as per Australian Standards AS 3634 [33]. Therefore, for the 3-speed pump investigated in this study, the high speed setting (2850 RPM) with the throttle valve fully open is defined as the Business as Usual (BAU) case for the operation of the test system.

For all pump speeds and flow rates shown in Fig. 3, the pump generated sufficient pressure to keep the vacuum relief valve on the solar collector closed. Hence, by adjusting the throttle valve between the minimum and fully closed position it is possible to operate the system at all three pump speeds with sufficient pressure to keep the vacuum relief valve closed.

## 6. Modelled solar pool collector performance under lower flow conditions

In order to characterise the performance of the unglazed solar pool collector, the fixed ambient weather parameters were assumed based on the test conditions as per International Standard ISO 9806 [51]. The collector inlet water temperature was set equal to the ambient temperature and the sky temperature was estimated to be 10°C for clear sky conditions [42]. Table 3 below shows all the parameters used in the simulation.

**Table 3 Parameters used for modelling the solar pool collector performance.**

| | |
|---|---|
| Solar irradiance | 800 W $m^{-2}$ |
| Ambient temperature | 25°C |
| Wind velocity | 3 m $s^{-1}$ |
| Collector inlet water temperature | 25°C |
| Sky temperature | 10°C |
| Collector tubing internal diameter | 4.3 mm |
| Collector tubing external diameter | 7.7 mm |
| Collector tubing surface area | 20.5 $m^2$ |
| Collector solar absorption [54] | 0.94 |
| Collector emissivity [55] | 0.91 |
| Collector tubing surface roughness [56] | 0.003 mm |
| Collector tubing coefficient of conductance (Polyethylene HD) [57] | 0.45 W $m^{-1}$ $K^{-1}$ |
| Thermal conductivity of water [58] | 0.598 W $m^{-1}$ $K^{-1}$ |

With the parameters provided in Table 3, the heat removal factor ($F_R$) and the temperature rise ($\Delta T$) of the solar collector under steady state conditions were calculated using the approach of Duffie and Beckman [30]. Fig. 4 below shows the logarithmic scale plot of the heat removal factor ($F_R$) and the temperature rise ($\Delta T$) of the solar collector under investigation against $\dot{m}/A_C$ varying from 0.0001 to 1.0 kg $s^{-1}$ $m^{-2}$.

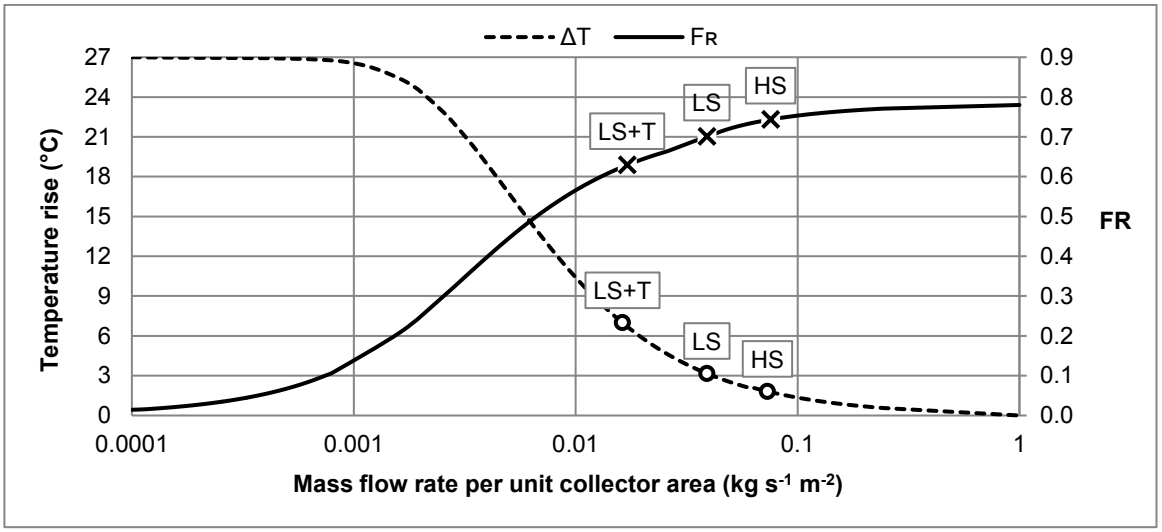


**Fig. 4. Plot of the modelled heat removal factor (FR) and temperature rise (□T) of the solar collector. Three FR values (X) and temperature rise values (O) are shown for mass flow rate per unit collector area corresponding to high pump speed with throttle valve fully opened (HS – 93 L/min (0.076 kg s$^{-1}$ m$^{-2}$)), low pump speed and minimum throttle (LS – 51 L/min (0.041 kg s$^{-1}$ m$^{-2}$)), and under low pump speed with the throttle valve partially throttled (LS+T – 20 L/min (0.016 kg s$^{-1}$ m$^{-2}$)).**

As can be seen from Fig. 4, for values of $\dot{m}/A_C$ > 0.1 kg s$^{-1}$ m$^{-2}$, the temperature rise ($\Delta T$) approaches zero while the heat removal factor (FR) tends towards its maximum value. On the other hand, for values of $\dot{m}/A_C$ < 0.002 kg s$^{-1}$ m$^{-2}$, the temperature rise tends towards its maximum value (in this case approximately 27°C) while the heat removal factor approaches zero. It is also important to note that the collector heat output is reduced by approximately 5% when the pump is switched from high speed (2850 RPM) (throttle valve fully opened) to low speed (2000 RPM) with the throttle valve at minimum throttle, as FR drops from 0.74 to 0.70. Also, the collector performance is not heavily penalized when the throttle valve is partially throttled with the pump operating at low speed as FR is only reduced by 16% in comparison to that of high speed operation (from 0.74 to 0.62). This implies that operating the system at lower values of $\dot{m}/A_C$ may be feasible as the reduction in heat output could be compensated for by extending the system running time of the pump. Also seen is that the heat output barely increases for $\dot{m}/A_C$ higher than 0.08 kg s$^{-1}$ m$^{-2}$, which is supported by the Australian Standards AS 3634 [33].

## 7. Experimental Results

### 7.1 Operating the solar collector at varying pump speeds

The solar pump was operated under different speeds on three consecutive days with similar weather conditions in order to analyse the effects on the system performance. Note that the throttle valve remained at the minimum throttle position for the low pump speed and fully opened at medium and high speeds. This ensured the vacuum relief valve remained closed and the highest achievable flow rate at each speed was obtained. In this section of the paper, the energy performance of the system is analysed in terms of the rate of energy coefficient of performance (COPr), which is the ratio of the rate of heat output from the solar collector to the electrical power supplied to the solar pump:

$$COP_r = \frac{\dot{Q}_u}{\dot{W}_{pump}} \qquad (14)$$

The rate of heat output ($\dot{Q}_u$) and COP$_r$ are plotted against the measured solar irradiance as shown in Fig. 5. The corresponding experimental uncertainties are given in Table 7 but not presented in Fig. 5 since the error bars are smaller than the markers, making the figure less clear to read. Both $\dot{Q}_u$ and COP$_r$ depend essentially linearly on the solar irradiance. Note that the rate of heat output was only marginally reduced when the pump was switched from high speed to low speed. This can also be seen from Fig. 4 as the heat removal factor has a minor drop from 0.74 to 0.70. The COP$_r$ of the system on the other hand, increased by around 2.8 times for a given solar irradiance when $\dot{m}/A_C$ was reduced from 0.076 kg s$^{-1}$ m$^{-2}$to 0.041 kg s$^{-1}$ m$^{-2}$, which is similar to the values reported by Cunio and Sproul [28].

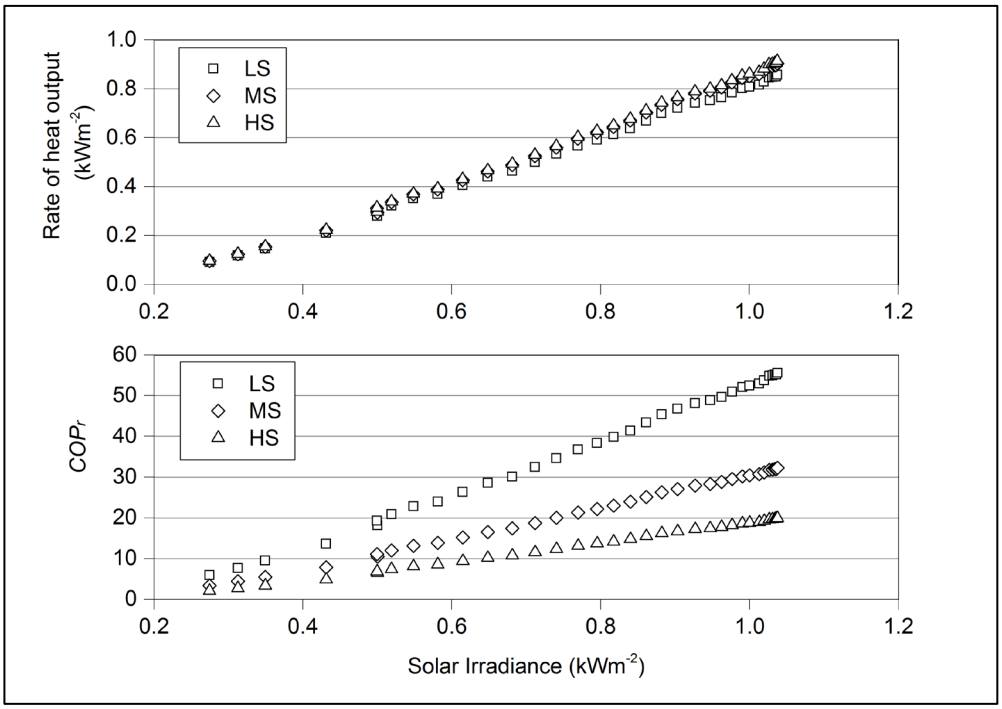


**Fig. 5. Comparison of rate of heat output (top figure), and coefficient of performance (bottom figure) for the system running under the following conditions: high pump speed with throttle valve fully opened (HS – 93 L/min (0.076 kg $s^{-1}$ $m^{-2}$)), medium pump speed with throttle valve fully opened (MS – 75 L/min (0.061 kg $s^{-1}$ $m^{-2}$)), and low pump speed (LS – 51 L/min (0.041 kg $s^{-1}$ $m^{-2}$)) with throttle valve set to the minimum throttle position.**

As the rates of heat output from the collector at the tested pump speeds are similar, when the pump speed is lowered, the higher $COP_r$ is due to reduced pump power. From high speed to low speed operation the magnitude of the $COP_r$ increased by about 2.8 times, and the pump energy was significantly reduced by nearly 64%. This was achieved by simply switching the pump to low speed without any other changes to the existing system.

### 7.2 TRNSYS model validation and tuning

The data collected over the entire experimental period (24 days at low speed, 7 days at medium speed and 7 days at high speed) was used to validate the steady state solar collector and swimming pool model, by following the steps below:

The initial simulation results were based on the theoretical values of the parameters outlined in Section 4 for both the solar collector model and the swimming pool model.

The simulation results obtained using the theoretical parameters were compared with the experimental data. The goodness of fit was assessed using the mean bias error (*MBE*), the root-mean-squared-error deviation (*Cv-RMSE*) and the coefficient of determination ($R^2$) [59].

Based on the statistical analysis results, the thermal model were tuned in order to achieve the optimum fit.

### 7.3 The solar collector model validation and tuning

The simulated values in TRNSYS were compared against the measured outlet water temperature and the rate of heat output from the collector, which was calculated using:

$$\dot{Q}_u = \dot{m} C_p (T_{out} - T_{in}) \qquad (15)$$

Figure 6 presents the plot of modelled rate of heat output ($\dot{Q}_{u\text{Modelled}}$) from the collector against the measured values ($\dot{Q}_{u\text{Measured}}$). An $R^2$ value of 0.97 indicates that the model describes the experimental data well.

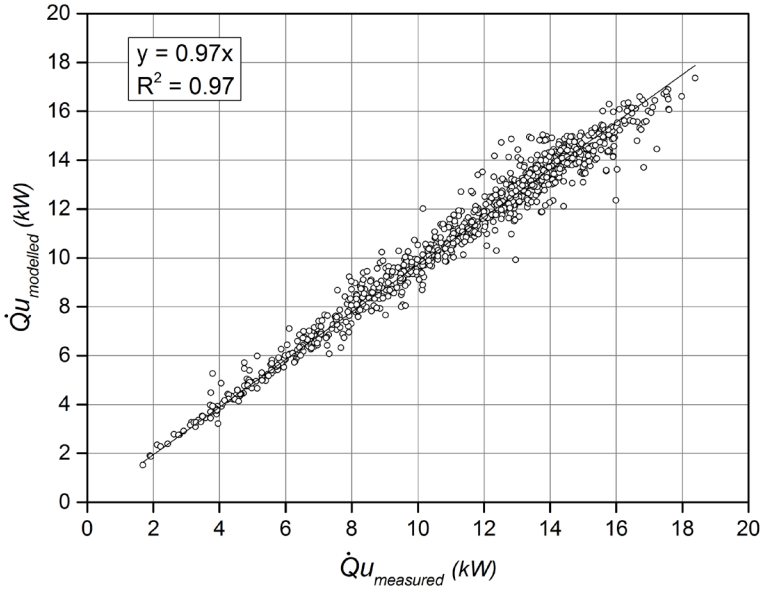


**Fig. 6 Plot of modelled rate of heat output of the solar collector against the experimental data (data set of 974 points).**

Following steps 1 & 2, the initial theoretical parameters produced modelled results with a MBE of -2.50% and -0.50% for $\dot{Q}_u$ and $T_{out}$ respectively (Table 4), indicating a reasonable match between the modelled and experimental data. However, the negative MBE implies that the model was slightly underestimating the actual heat output, which could possibly be caused by some additional heat losses that were considered in the model.

**Table 4 Statistical analysis results of the steady state collector model with initial theoretical parameters (data set of 974 points).**

| | Data resolution | *MBE* | *Cv-RMSE* | $R^2$ |
|---|---|---|---|---|
| $\dot{Q}_u$ | 10 minute | -2.50% | 8.4% | 97.0% |
| $T_{out}$ | | -0.50% | 1.8% | 98.6% |

As discussed in section 4.1, the temperature difference between the roof and collector surface was initially assigned a constant value (5 K) using previous data from the literature. However, it was identified as a variable to be tuned in the final fit (Step 3 above) given the complexity of the roof profile and the collector. Only the temperature difference between the collector surface and the roof was varied, the other theoretical values used in the model for the pool solar collector were kept constant. The detailed statistical results are shown in Table 5. It was found that the optimum fit was achieved when the average temperature difference between the collector and the roof was 2.14 K, yielding an *MBE* of zero and a *Cv-RMSE* of 7.6%.

**Table 5 Statistical results of the solar collector model fitting by varying the temperature difference between the collector and the roof ($T_c - T_{roof}$) (data set of 974 points with 10 min resolution).**

| $T_c$-$T_{roof}$ | $\dot{Q}_u$ | | | $T_{out}$ | | |
|---|---|---|---|---|---|---|
| | *MBE* | *Cv-RMSE* | $R^2$ | *MBE* | *Cv-RMSE* | $R^2$ |
| 5 K | -2.50% | 8.4% | 97% | -0.50% | 1.8% | 98.6% |
| 3 K | -0.76% | 7.7% | 97% | -0.11% | 1.6% | 98.6% |
| 2.14 K | 0.00% | 7.6% | 97% | -0.01% | 1.6% | 98.6% |
| 1 K | 1.01% | 7.7% | 97% | 0.20% | 1.6% | 98.6% |

### 7.4 The swimming pool model validation and tuning

A simple model of the open-air pool and its surrounding objects was built in Sketchup to simulate the shading percentage of the pool during the experimental period. Fig. 7 below shows a rough comparison of the real time camera images of the pool with the simulated snapshots in Sketchup on 18th March 2016. It can be seen that the Sketchup model presents a good estimation of the real pool shading percentage. Therefore, it was used to determine the pool shading factors over the required period (Table 6).

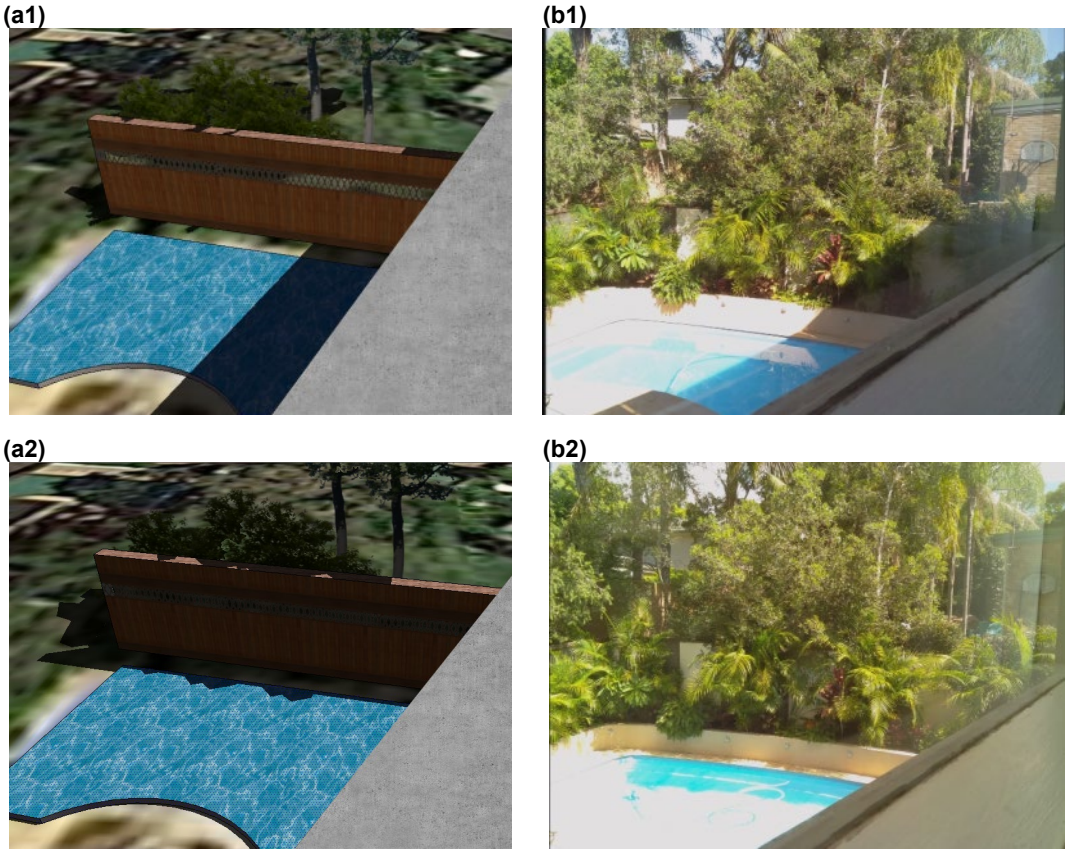


**Fig. 7 Comparison of the simulated snapshots obtained in Sketchup (a) against the real time camera images (b) taken at 10:50 AM and 12:50 PM on 18/03/2016.**

**Table 6 Modelled monthly average shading factors of the tested swimming pool.**

| | Monthly average shading factor |
|---|---|
| October | 57% |
| November | 41% |
| December | 31% |
| January | 28% |
| February | 44% |
| March | 57% |

Once the solar collector model was validated and tuned with the best fit against the experimental data, the swimming pool model validation was undertaken following the same procedures given in section 7.2. Table 7 shows the different expressions of the evaporative heat transfer coefficient of the pool summarized by Ruiz and Martínez [49] and Buonomano and De Luca [47]. These seven, different evaporative heat transfer coefficients were compared using the TRNSYS model against the experimental data. The statistical results are also presented in Table 7. It can be seen that the expression provided by Richter [50] gives the best agreement between the modelled and measured results with an *MBE* of -0.36% and *Cv-RMSE* of 0.6%. This is in agreement with Ruiz and Martínez [49] as the heat loss coefficient reported by Richter [50] also produced the best overall fit to their experimental data.

**Table 7 Statistical analysis results of the swimming pool model with different evaporative heat transfer coefficients (data set of 974 points). Data resolution for all cases is 10 minutes.**

| *Literature* | *Evaporative heat transfer coefficient ($W\ m^{-2}\ kPa^{-1}$)* | | *Pool temperature* | | |
|---|---|---|---|---|---|
| | | | *MBE* | *Cv-RMSE* | *$R^2$* |
| Lam and Chan [48] | $h_{evap} = 4.08 + 4.28V_{W_p}$ | (16) | 0.83% | 1.1% | 98.6% |
| McMillan [60] | $h_{evap} = 36 + 25V_{W_p}$ | (17) | -1.55% | 1.2% | 98.7% |
| Richter [50] | $h_{evap} = 42.3 + 56.6V_{W_p}^{0.5}$ | (18) | -0.36% | 0.6% | 98.7% |
| Standards Australia [33] | $h_{evap} = 50.6 + 66.9V_{W_p}$ | (19) | -2.88% | 2.6% | 98.1% |
| Smith et al. [61] | $h_{evap} = 63.8 + 66.9V_{W_p}$ | (20) | -3.29% | 3.4% | 98.0% |
| Rohwer [62] | $h_{evap} = 85 + 50.8V_{W_p}$ | (21) | -3.14% | 3.3% | 97.8% |
| ASHRAE [63] | $h_{evap} = 89 + 78.2V_{W_p}$ | (22) | -3.93% | 4.1% | 97.7% |

Figure 8 presents sample results of the model validation processes for the three pump speeds for both sunny days and days with intermittent clouds. Figure 8 along with the statistical analysis presented in Table 10 and Table 12 show good agreement between the modelled results and the measured data, validating the collector and pool model and hence, the model was used for further simulations.

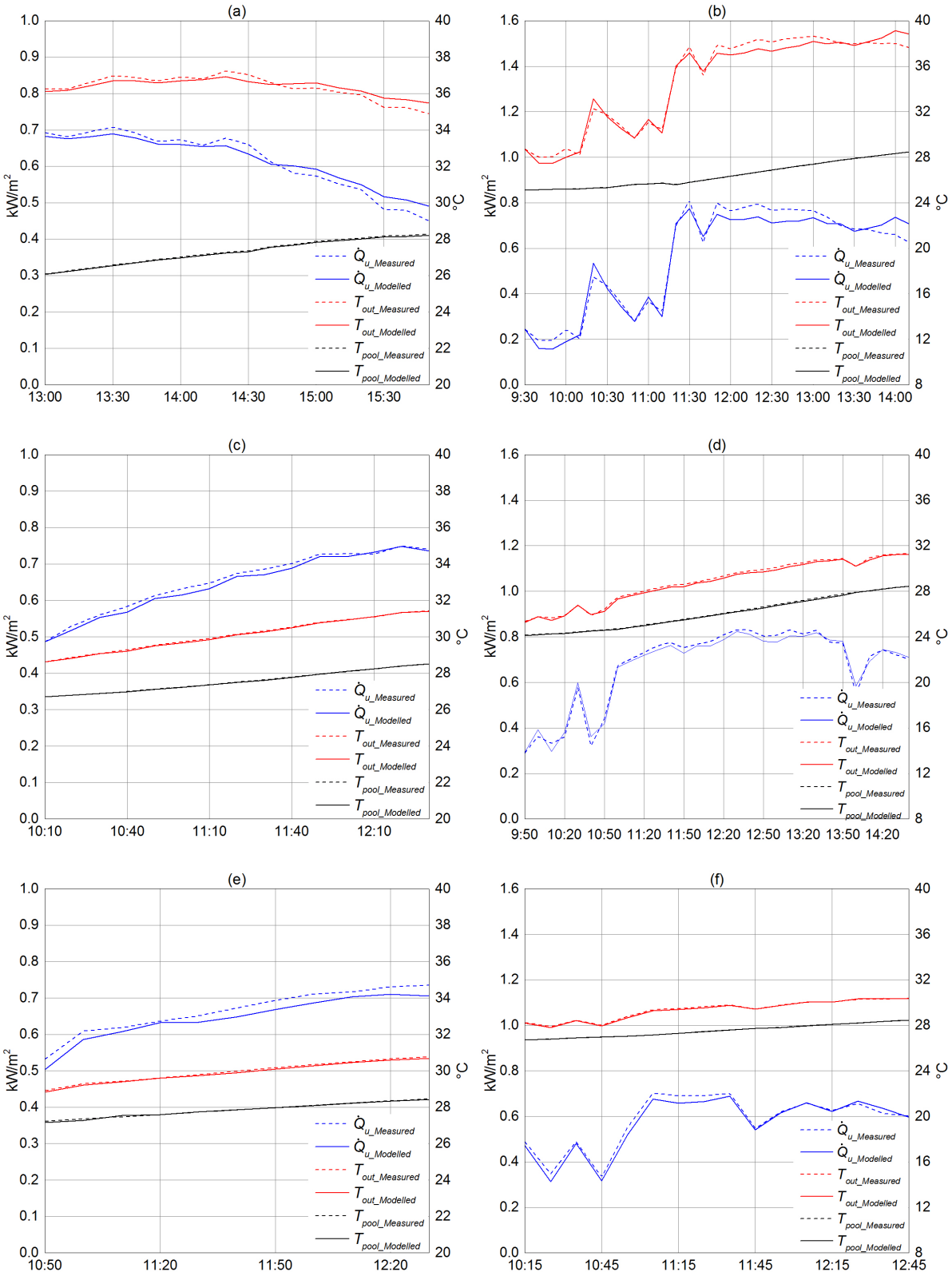


**Fig. 8 Comparison of experimental and modelled data for typical sunny days (LHS figures) and cloudy days (RHS figures) for various values of $\dot{m}/A_C$: a) and b) 0.041 kg s$^{-1}$ m$^{-2}$, c) and d) 0.061 kg s$^{-1}$ m$^{-2}$, and for e) and f) 0.076 kg s$^{-1}$ m$^{-2}$.**

## 8. TRNSYS simulations of the whole of solar pool heating system under lower flow and low pump speed conditions

### 8.1 Swimming pool with no solar collector heating

Having validated the TRNSYS model for the collector and the pool against experimental data, the whole of system model was used to simulate the solar pool heating system for the period of October to March (182 days), which represents the summer period in Sydney. The initial pool temperature was set equal to the mean ambient temperature of September which was obtained from the data collected at the nearest observation site (Terrey Hills) available from the Bureau of Meteorology (BOM [64]). The TMY2 weather data file for Sydney provided by TRNSYS [65] along with the real pool shading factors (Table 11) of the test pool (from the Sketchup model) were used.

Fig. 9 shows the daily average heat exchange of the swimming pool with no solar pool heating. It can be seen that the total pool heat losses (sum of $Q_{conv}$, $Q_{rad}$, and $Q_{evap}$) is approximately balanced by the pool heat gains due to the absorption of solar irradiance ($Q_{sol}$); thus, the average pool temperature generally follows the trend of the ambient air temperature. Notice that the small discrepancy between the calculated values of the total pool heat gains and losses is only 2%, which may possibly be due to ignoring the pool conduction loss to the ground.

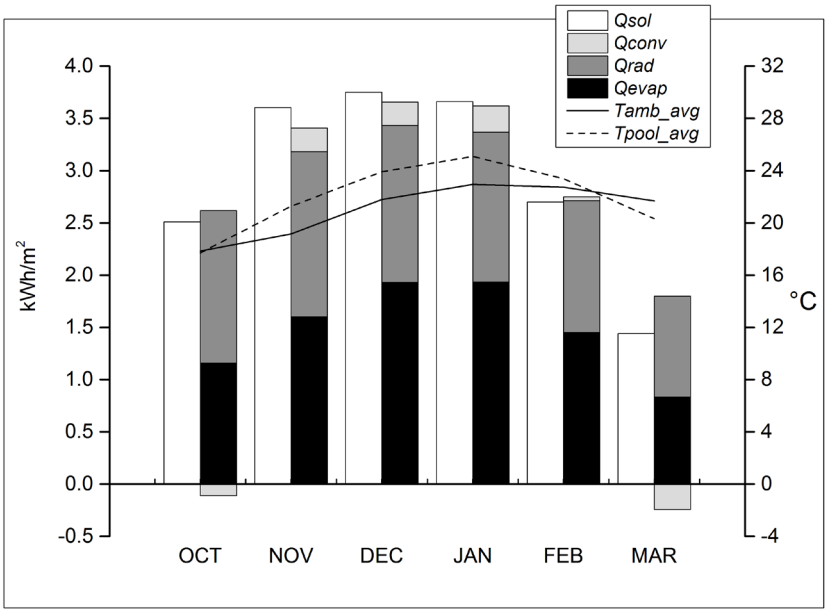


**Fig. 9. Swimming pool daily average net heat exchange from October to March with no solar pool heating.**

It can also be seen from Fig. 9 that the heat losses due to evaporation and radiation make up the majority of the heat losses from the pool. As the convective heat loss depends on the difference between the pool and the ambient temperature, its value is relatively small over the whole period provided that the average pool temperature is close to the ambient temperature. The convective heat loss is negative during October and March due to the lower pool temperature and can be considered as extra heat gain from the ambient.

### 8.2 Swimming pool with solar collector heating – optimal flow rate for 1 degree pool temperature rise

As previously discussed, operating the solar pump under low speed (2000 RPM) has the potential to achieve significant pump energy savings. For the experimental setup described above, the solar pool heating system was capable of operating under low speed with the throttle valve partially throttled (lower flow). The electrical energy supplied to the pump ($\boldsymbol{W_{pump}}$) required for achieving a 1°C pool temperature rise with the solar pool heating system operating at high and low pump speeds is presented in Fig. 10.

This was calculated based on the experimentally measured electrical power supplied to the pump ($\dot{W}_{pump}$) and the pump running time obtained by TRNSYS simulations over the corresponding flow rate ranges. Also shown is the associated coefficient of performance (COP). Note that the COP was calculated based on Eqn. 1, i.e. in terms of energy, not rate of energy. For this calculation it was assumed that the heat losses of the pool were offset by the direct solar heat gains (Fig. 9) and stable ambient conditions were assumed as shown in Table 8.

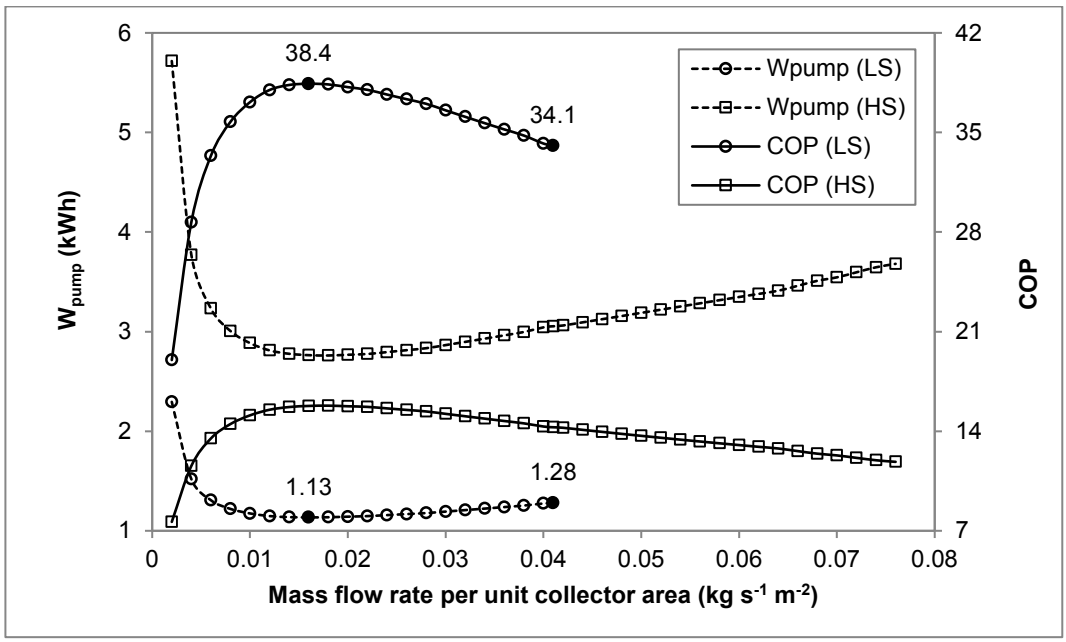


**Fig. 10. Electrical energy supplied to the pump for a 1°C pool temperature increase and COP as a function of mass flow rate per unit collector area for high and low pump speeds (fixed ambient conditions).**

It is clear that the low pump speed uses considerably less energy than the high pump speed to achieve the 1°C increase. When $\dot{m}/A_C$ is below 0.01 kg s$^{-1}$ m$^{-2}$, the pump energy increases significantly due to the reduction in the motor/pump efficiency as well as longer running times due to the loss in thermal output at lower $\dot{m}/A_C$ (shown in Fig. 4). In addition, the lowest pump energy consumption (1.13 kWh) and highest COP (38.4) for the test system occur at a value for $\dot{m}/A_C$ of 0.016 kg s$^{-1}$ m$^{-2}$ (low pump speed operation with the throttle valve partially throttled), which is approximately 40% of the value of $\dot{m}/A_C$ at low speed with the throttle valve at the minimum throttle position (0.041 kg s$^{-1}$ m$^{-2}$) and only 20% of the value of $\dot{m}/A_C$ at high speed with the throttle valve fully opened (0.076 kg s$^{-1}$ m$^{-2}$). This mass flow rate per unit collector area is about 50% lower than the minimum value specified by the International standard ISO/TR 12596 [32] and the Australian Standard AS3634 [33].

In comparison to the flow rates reported in the literature, the optimal value of $\dot{m}/A_C$ identified here is very close to those adopted by Sodha and Kumar [23] and Dongellini and Falcioni [29], which were 0.018 kg s$^{-1}$ m$^{-2}$ and 0.015 kg s$^{-1}$ m$^{-2}$ respectively. From Fig. 10, for low pump speed operation, the optimal range for $\dot{m}/A_C$ can be found as 0.01 kg s$^{-1}$ m$^{-2}$ to 0.03 kg s$^{-1}$ m$^{-2}$ for a solar pool heating system in order to achieve maximum COP. This supports the initial work done by Cunio and Sproul [28] and is in agreement with the lowest values of $\dot{m}/A_C$ reported in the literature [19, 23, 26-29].

### 8.3 Swimming pool with solar collector heating – long-term simulation

The running time of the pump however, is not easy to calculate as it is affected by changes in the pool temperature, local weather conditions, and site factors such as the pool shading profile. Thus, the actual system performance and energy saving potentials at this specific flow rate will be investigated more accurately by considering the thermal behaviour of the swimming pool based on real weather conditions over the whole system running period.

For the long term simulations, the solar pump was assumed to start when the collector outlet water temperature exceeded

the inlet temperature by 10°C. In addition, it automatically turned off when the pool temperature reached 28°C and re-started when the pool temperature dropped to 26°C. Only the pool temperatures from 10 am to 7 pm were considered, as this is the timeframe during which the pool is normally used.

Fig. 11 shows the average daily pool temperature and pump energy consumption for the system running under low speed (2000 RPM) with the throttle valve partially throttled (0.016 kg $s^{-1}$ $m^{-2}$) and the high speed (2850 RPM) BAU case with the throttle valve fully opened (0.076 kg $s^{-1}$ $m^{-2}$). It is clear that running the solar pool heating system at lower flow and low pump speed only uses around 40% of the energy usage of the high speed BAU case, without actually changing the average pool temperature.

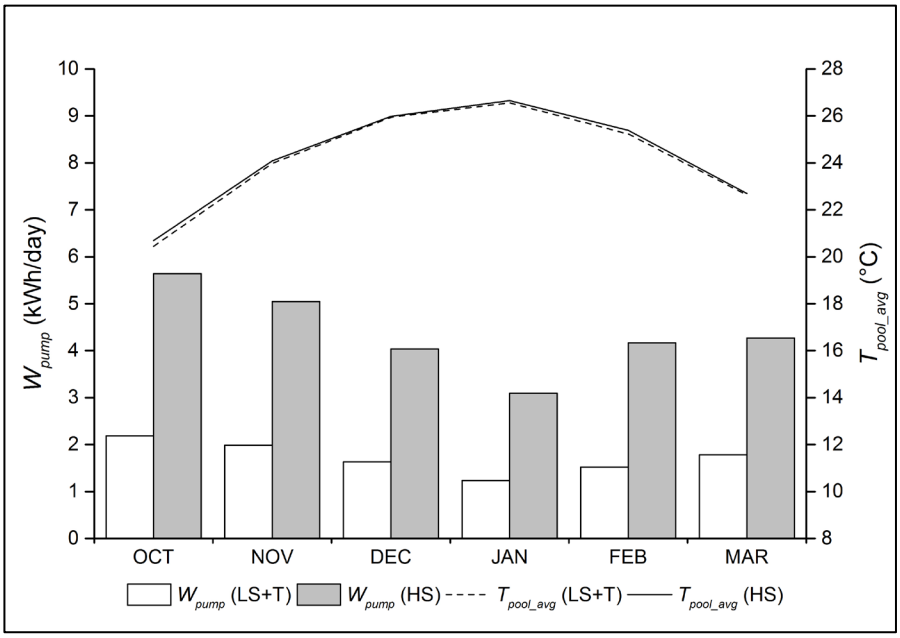


**Fig. 11. Daily average pool temperature and electrical energy supplied to the pump during the period of 10 am and 7 pm for the solar pool heating system operating under low pump speed with the throttle valve partially throttled (LS+T – 20 L/min (0.016 kg $s^{-1}$ $m^{-2}$)), and high pump speed with the throttle valve fully opened (HS – 93 L/min (0.076 kg $s^{-1}$ $m^{-2}$)) from October to March.**

Although the lower efficiency of the collector must be compensated by longer running times, there is still a net reduction in pump electricity consumption. Simulation results show that the system operating at low speed with the throttle valve partially throttled needed on average 6 hours to complete the same daily heating task, which is approximately 1.5 hours more than the high speed BAU case. Fig. 12 shows the pool heat gain per unit pool area due to the absorption of solar irradiance ($Q_{sol}$) and from the solar collector ($Q_u$) under low and high speeds over the October to March period. The difference of the collector heat output for low and high speed operation is relatively small and can therefore be neglected. Also it is clear that the majority of the pool heat gains for the partially shaded pool is due to the direct solar irradiance, which is in agreement with the findings reported by Hahne and Kübler [25].

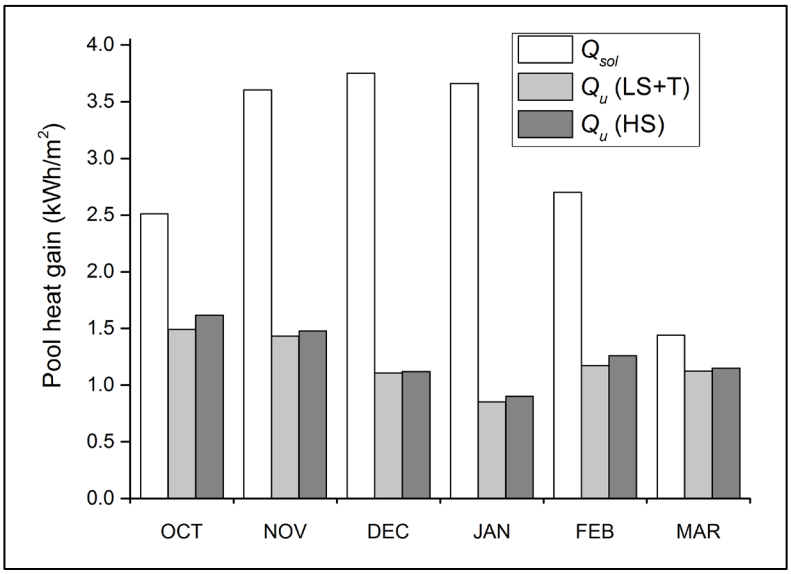


**Fig. 12. Daily average pool heat gains for the solar pool heating system operating under low pump speed with the throttle valve partially throttled (LS+T – 20 L/min (0.016 kg s$^{-1}$ m$^{-2}$)), and high pump speed with the throttle valve fully opened (HS – 93 L/min (0.076 kg s$^{-1}$ m$^{-2}$)) from October to March.**

Fig. 13 below shows the number of days when the average pool temperature falls within various temperature ranges. Assuming a minimum swimmable water temperature of 26°C as recommended by the DOE [66], there are only 5 days that meet this criterion for a natural pool with no solar collector heating. However, with the operation of the solar pool heating system, approximately 40 days have an average pool temperature above 26°C which indicates a longer swimming season. The graph also shows that reducing the flow rate by operating the pump at low pump speed with the throttle valve partially throttled results in a similar average pool temperature distribution.

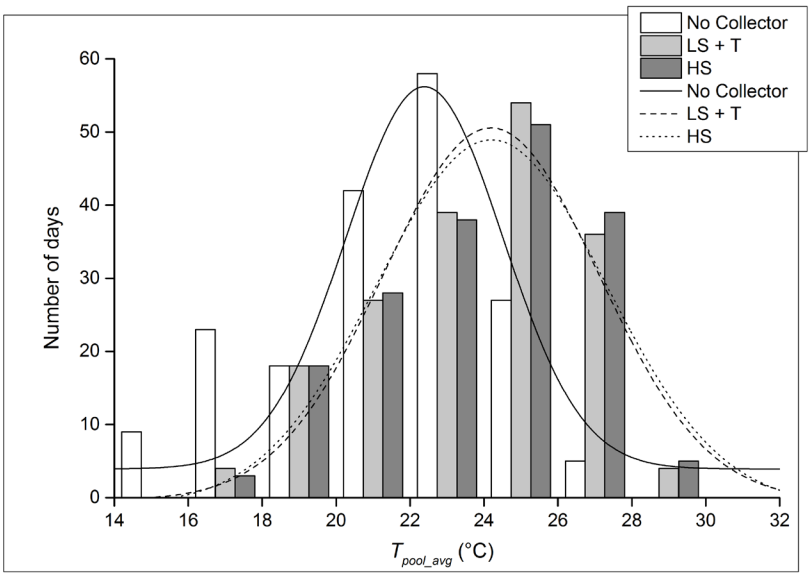


**Fig. 13. Histogram of the average pool temperature with no collector heating and with solar pool heating system operating at low pump speed with the throttle valve partially throttled (LS+T – 20 L/min (0.016 kg s$^{-1}$ m$^{-2}$)), and high pump speed with the throttle valve fully opened (HS – 93 L/min (0.076 kg s$^{-1}$ m$^{-2}$)) from October to March.**

This confirms that for this system, operating with a lower value of $\dot{m}/A_C$ of 0.016 kg s$^{-1}$ m$^{-2}$ does not materially affect the thermal comfort of the swimming pool. Importantly, operating the pump at its lowest speed (2000 RPM) with the throttle

valve partially throttled achieves nearly a 60% pump energy saving, compared to the high speed BAU case (2850 RPM).

Furthermore, the system coefficient of performance (COP), defined as the ratio of the thermal energy delivered to the pool to the electrical energy supplied to the pump over the entire simulation period, has increased from approximately 9.8 (high pump speed) to 24.7 (low pump speed). Correspondingly, the average thermal energy operational cost (electricity cost divided by thermal input to the pool) has reduced from approximately $0.033/kWh to $0.013/kWh based on the flat rate electricity tariff ($0.323/kWh) provided by Energy Australia [67]. This indicates a significant improvement of the energy efficiency and cost effectiveness of operating the solar pool heating system.

It should be noted that the pre-determined flow rate or the throttling position will vary across different systems, considering the various local conditions and different system operating scenarios. Additionally, utilizing a throttle valve to restrict the water flow at low pumping speed is considered as a cost-effective option for any system aiming for energy saving as this can be achieved with existing systems.

### 8.4 Swimming pool with solar collector heating – collector area considerations

Given that significant energy savings can be obtained whilst achieving similar pool thermal conditions, it is also important to investigate the effects of various solar collector areas on the system performance and the pool thermal condition under the lower flow and low pump speed operation. Following the same methods presented in section 8.3, the system performance was modelled in TRNSYS under various collector to pool area ratios, which were 0 (no collector), 0.6 (Business as Usual), 1, and 1.5. The area of the test collector is approximately 60% of the pool area, which meets the requirements as per the Australian Standards AS 3634 [33]. This is therefore defined as the BAU collector area in this study.

Fig. 14 shows the average pool temperature for different typical collector to pool area ratios under lower flow, low pump speed conditions. The average pool temperature with no solar collector during the summer months stays at around 25°C, i.e., it does not reach the swimmable temperature of 26°C. Using a solar collector with a BAU area (60% of the pool surface area), the average pool temperature is increased on average by around 2°C. In this case, the pool temperature remains higher than 26°C from early December until early January. When the collector area is the same as the pool surface area, the average water temperature increases by an additional 1°C, extending the swimming season even further. A further rise in the collector to 1.5 times the pool surface area only increases the water temperature slightly during cooler months, but not much in peak summer.

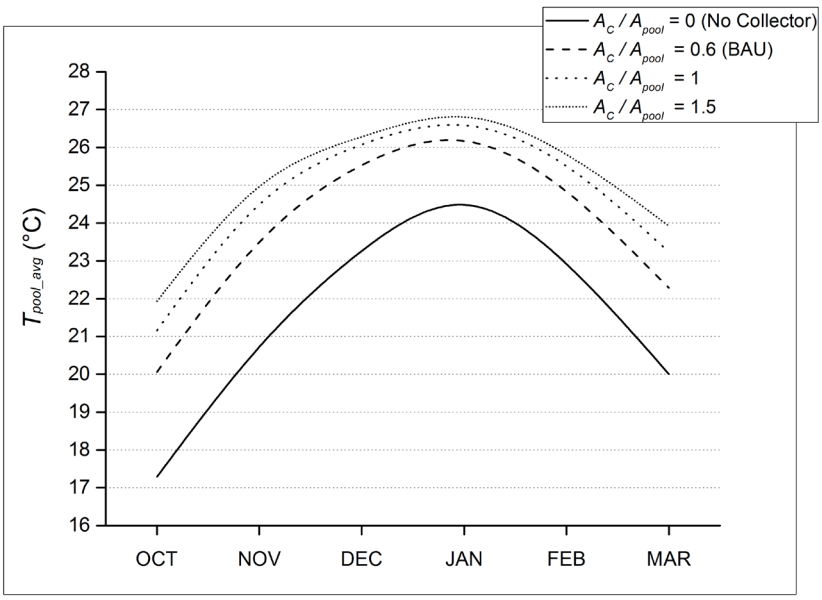


**Fig. 14. Average pool temperature at low pump speed with the throttle valve partially throttled (LS+T – 20 L/min (0.016 kg $s^{-1}$ $m^{-2}$)) for different collector to pool area ratios – partially shaded pool.**

Fig. 15 shows the distribution of the average pool temperatures for different collector areas from October to March. An

increase in the collector to pool area ratio from 0.6 to 1 results in 27 extra days of water temperature over 26°C. Furthermore, the average daily system running time is reduced by approximately 1 hour per day (from 6 hour/day to 5 hours/day). In terms of an even larger collector area (1.5 times the pool area), a 10 day longer swimming period is achieved with a further drop in the system running time of 0.5 hours. This represents a total of 37 days longer swimming period for about the same daily running time in comparison to the BAU case (high speed operation with standard collector to pool area ratio of 0.6). The appropriate collector area will vary across different pool heating systems considering the various geolocations, site specific parameters and individual pool operational requirements, and the minimum acceptable pool temperature.

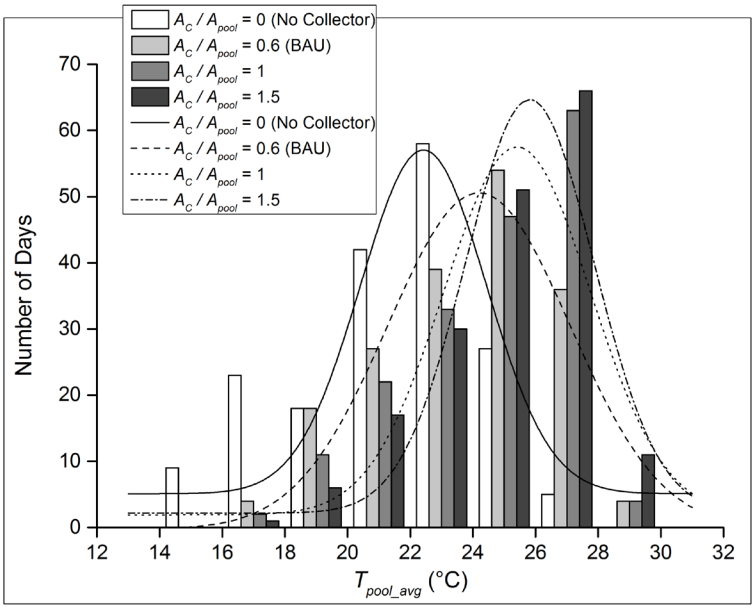


**Fig. 15. Histogram of the average pool temperature at low pump speed with the throttle valve partially throttled (LO + T – 20 L/min (0.016 kg $s^{-1}$ $m^{-2}$)) for different collector to pool area ratios – partially shaded pool.**

## 8.5 Energy saving and carbon emission reductions

This work has shown that operating a solar pool heating system under lower flow, low pump speed conditions is feasible and can lead to a significant amount of pump energy savings. Hence, it is worthwhile to consider the potential contributions towards reducing electrical energy use in Australia.

Table 8 presents the estimated yearly electricity savings and carbon emission reductions by operating residential solar pool heating systems under lower flow, low pump speed conditions across Australia. The key assumptions are: 1) the proportion of the pools heated by solar collectors in Australia is 27% [10, 11]; 2) the average daily energy use by a solar pool heating system is 6 kWh/day [12]; 3) the annual operating period of the swimming pool is 182 days (From October to March); and 4) the pump energy saving proportion is 60% when the solar pool heating system is operated at lower flow conditions and utilising a low pump speed (e.g. 2000 RPM).

**Table 8 Calculations of yearly electricity savings and carbon reductions.**

| State | Number of pools [1] | Number of pools with solar collectors | Electricity emission factors (kg $CO_2$-e/kWh) [68] | Annual energy savings (GWh/yr) | Annual carbon reduction (kt $CO_2$-e) |
|---|---|---|---|---|---|
| New South Wales | 337,600 | 91,152 | 0.96 | 59.7 | 57.3 |
| Queensland | 312,300 | 84,321 | 0.94 | 55.2 | 51.9 |
| Victoria | 146,400 | 39,528 | 1.19 | 25.9 | 30.8 |
| Western Australia | 129,300 | 34,911 | 0.79 | 22.9 | 18.1 |
| South Australia | 57,100 | 15,417 | 0.64 | 10.1 | 6.5 |
| Northern Territory | 21,400 | 5,778 | 0.77 | 3.8 | 2.9 |
| Capital Territory | 8,100 | 2,187 | 0.96 | 1.4 | 1.4 |
| Tasmania | 6,700 | 1,809 | 0.13 | 1.2 | 0.2 |
| **Total** | | | | **180.2** | **147.2** |

As can be seen from Table 8, if all solar pool heating systems in Australia were operating at a lower flow rate and low pump speed, this could save approximately 180 GWh of electricity per year, which corresponds to approximately 150 kilotonnes of carbon emission abatement. This electricity reduction represents approximately 9% of the total projected electricity usage of Australian swimming pools in 2016 [7]. The projected electricity consumption of the residential sector in Australia for 2016 is approximately 230 PJ, hence, operating all solar pool heating systems at a lower flow rate and low pump speed could reduce the energy use of the residential sector by approximately 0.3%.

## 9. Conclusions

The feasibility and energy saving potential of operating a commercially available solar pool heating system under lower flow, low pump speed conditions were investigated. Experimental data was used to validate a theoretical model for a solar pool collector and an open-air swimming pool. The results obtained show that the theoretical collector parameters gave good agreement against the measured values, with a *MBE* close to zero and a $R^2$ greater than 95% for both the rate of heat output ($\dot{Q}_u$) and the outlet water temperature ($T_{out}$). The model achieved the best overall fitting results with the average temperature difference between the collector and roof being 2.14 K. The theoretical parameters for the swimming pool model showed a good fit to the experimental data with a *MBE* = -0.36%, *Cv-RMSE* = 0.6, and $R^2$ = 98.7%.

This study presents for the first time the flow rate optimization for solar pool collectors based on maximising the system COP (energy ratio). Results show that the optimal mass flow rate per unit collector area is 0.016 kg $s^{-1}$ $m^{-2}$, achieved using a 3-speed pump, operating at its lowest speed (2000 RPM) and partially throttling the throttle valve. Note this optimal flow rate is approximately half of the minimum value of 0.03 kg $s^{-1}$ $m^{-2}$, recommended by the International standard ISO/TR 12596 and the Australian Standard AS3634 [32, 33]. From our research, a range of 0.01 – 0.03 kg $s^{-1}$ $m^{-2}$ is proposed for $\dot{m}/A_C$ for unglazed solar pool collectors in order to achieve the highest COP.

This paper also for the first time, addresses the fundamental hydraulic theory of the typical residential solar pool heating systems. For the high speed BAU case, when operated at a mass flow rate per unit collector area ($\dot{m}/A_C$) of 0.076 kg $s^{-1}$ $m^{-2}$, the pump produced a pressure of 144 kPa. By contrast, our approach (lower flow, low pump speed) operated at 0.016 kg $s^{-1}$ $m^{-2}$ produced a pump pressure of 74 kPa. As for pool filtration systems, lower flow rates result in lower frictional losses and therefore lower pump pressure and energy [17, 38]. This approach also works for solar pool heating systems, however the pressure developed by the solar pump has to be greater than a certain level (Eqn. 13) for the system to operate with the vacuum relief valve closed. This was achieved using the throttle valve to restrict the flow rate, and hence ensuring the pressure of the pump is high enough to keep the vacuum relief valve remained closed at all times (Fig. 3). Notice that a throttle valve is a standard component of a typical solar pool heating system. Hence the addition of a low speed, energy saving pump would be a simple retrofit to any existing solar pool heating systems.

Since less pump pressure was required under lower flow condition in comparison to the BAU case, the optimized system achieved pump energy savings of approximately 60% and an average system COP of around 25 when the whole of system

was modelled over the entire swimming season. This is a significant improvement in energy efficiency when compared to the COP of around 9.8 for the high speed BAU case ($\dot{m}/A_C$ equal to 0.076 kg $s^{-1}$ $m^{-2}$) and also a significant improvement in comparison to a COP of 4.7 for typical air to water pool heat pumps at nominal conditions [69]. In addition, the approach described in this paper did not compromise the thermal comfort of the pool and only added 1.5 hours to the normal daily running time when compared to the high speed BAU case. This is not considered a significant issue given the improved COP and the significant pump energy savings, which minimizes the system operational cost. Further, with an increase of the collector to pool area ratio from 0.6 to 1.5, lower flow and low speed operation of the solar pool heating system added one month to the swimming period with the same daily running time in comparison to the BAU case – high speed operation with the standard collector area. The additional capital required for the larger collector could be paid back by the electricity savings obtained.

Based on the data provided by Ausgrid [12], for a solar pool heating system operating during the swimming period with the pump operated at low speed and lower flow, the daily pumping energy required could be reduced by 3.6 kWh/day. This represents a nearly 20% reduction of the average household electricity demand (19.2 kWh/day) in the greater Sydney region [4]. If all residential solar heated pools in Australia were retrofitted with this energy efficiency measure, the annual electricity demand of residential pools would be reduced by around 10% (180 GWh/year). This is equivalent to 150 kilotonnes of carbon reduction per year.

## Acknowledgements

This research was funded by the CRC for Low Carbon Living Ltd supported by the Cooperative Research Centres program, an Australian Government initiative. One of the authors (JZ) acknowledges the support of an APA scholarship with an additional financial support from the CRC for Low Carbon Living. The authors would also like to acknowledge the technical support from Dr Nicholas Shaw and Mr Mark Griffin, School of Photovoltaic and Renewable Energy Engineering, University of New South Wales.

## References

[1] ABS, Environmental Issues: Water use and Conservation, Australian Bureau of Statistics, Australian Government, 2010.
[2] DEE, Consultation Regulation Impact Statement - Swimming Pool Pumps, Department of the Environment and Energy, Commonwealth of Australia, 2016.
[3] A. Elnakat, J.D. Gomez, J. Roberts, M. Wright, Big data analysis of swimming pools' impact on household electric intensity in San Antonio, Texas, International Journal of Big Data Intelligence 2 (2015) 250-261.
[4] H. Fan, I.F. MacGill, A.B. Sproul, Statistical analysis of driving factors of residential energy demand in the greater Sydney region, Australia, Energy and Buildings 105 (2015) 9-25.
[5] P. Seebacher, Swimming Pools and Peak Load Demand Response, Energy Rating, A joint initiative of Australian, State and Territory and New Zealand, 2006.
[6] Ergon Energy, Demand Management Outcomes Report 2012/13, Ergon Energy Corporation Limited, 2013.
[7] EES, Energy use in the Australian residential sector 1986-2020, Energy Efficient Strategies Pty Ltd (EES). Department of the Environment, Water, Heritage and the Arts, Commonwealth of Australia, 2008.
[8] DEE, Quarterly Update of Australia's National Greenhouse Gas Inventory: March 2017, Department of the Environment and Energy, Commonwealth of Australia, 2017.
[9] G. Wilkenfeld, Swimming Pools - Energy Use and Impact on Peak Load, Energy Rating, A joint initiative of Australian, State and Territory and New Zealand Governments, 2009.
[10] G. Wilkenfeld, Swimming pools and electric space heating, prepared for the Australian Building Codes Board, Energy Policy and Planning Consultants, 2009.
[11] Woolcott Research and Engagement, Pool Pumps: An Investigation of Swimming Pool Pumps in Australian and New Zealand, A research report prepared for the Department of the Environment and Energy, Commonwealth of Australia, 2016.
[12] Ausgrid, Pool & Spa Guide - Swimming pool efficiency. https://www.ausgrid.com.au/-/media/Files/Customer-Services/Homes/Energy-Efficiency/Ausgrid-Swimming-Pool-brochure-2015.pdf, 2015 (accessed 2018 January 29th).
[13] D.A. Katsaprakakis, Comparison of swimming pools alternative passive and active heating systems based on renewable energy sources in Southern Europe, Energy 81 (2015) 738-753.
[14] L. Johansson, L. Westerlund, Energy savings in indoor swimming-pools: comparison between different heat-recovery systems, Applied Energy 70 (2001) 281-303.
[15] M.E. Kuyumcu, H. Tutumlu, R. Yumrutaş, Performance of a swimming pool heating system by utilizing waste energy rejected from an ice rink with an energy storage tank, Energy Conversion and Management 121 (2016)

349-357.
[16] D. Springer, F. Rohe, Field Studies of Two-Speed and PV-Powered Pumps and Advanced Controls for Swimming Pools, ACEEE Summer Study on Energy Efficiency in Buildings “Profiting from Energy Efficiency” (1996)
[17] A.B. Sproul. Design of PV powered, high efficiency pool pump systems. in ANZSES solar energy conference. 2005.
[18] Z. Hameiri, E.D. Spooner, A.B. Sproul, High efficiency pool filtering systems utilising variable frequency drives, Renewable Energy 34 (2009) 450-455.
[19] J.T. Czarnecki, Swimming pool heating by solar energy, Technical report No.TR19., CSIRO Division of Mechanical Engineering, Highett, Victoria, 1978.
[20] G.L. Morrison, E. Donnelly, Thermal performance of solar energy systems for swimming pools. School of Mechanical and Industrial Engineering, University of New South Wales, 1980.
[21] J. Cusido, J. Puigdomenech, An experimental solar system for swimming pool heating in Mediterranean climates, Solar & wind technology 3 (1986) 141-145.
[22] A. Dang, A parametric study of swimming pool heating—I, Energy Conversion and Management 26 (1986) 27-31.
[23] M. Sodha, A. Kumar, Solar heating of open swimming pools, International journal of energy research 12 (1988) 511-519.
[24] M. Singh, G. Tiwari, Y. Yadav, Solar energy utilization for heating of indoor swimming pool, Energy Conversion and Management 29 (1989) 239-244.
[25] E. Hahne, R. Kübler, Monitoring and simulation of the thermal performance of solar heated outdoor swimming pools, Solar Energy 53 (1994) 9-19.
[26] B. Molineaux, B. Lachal, O. Guisan, Thermal analysis of five unglazed solar collector systems for the heating of outdoor swimming pools, Solar Energy 53 (1994) 27-32.
[27] S. Medved, C. Arkar, B. Černe, A large-panel unglazed roof-integrated liquid solar collector—energy and economic evaluation, Solar Energy 75 (2003) 455-467.
[28] L.N. Cunio, A.B. Sproul, Performance characterisation and energy savings of uncovered swimming pool solar collectors under reduced flow rate conditions, Solar Energy 86 (2012) 1511-1517.
[29] M. Dongellini, S. Falcioni, A. Martelli, G.L. Morini, Dynamic simulation of outdoor swimming pool solar heating, Energy Procedia 81 (2015) 1-10.
[30] J.A. Duffie, W.A. Beckman, Solar engineering of thermal processes, 4th Edition. John Wiley & Sons, 2013.
[31] J. Baughn, M. Young, The calculated performance of a solar hot water system for a range of collector flow rates, Solar Energy 32 (1984) 303-305.
[32] ISO, ISO/TR 12596: 1995(E) Solar heating - Swimming-pool heating Systems - Dimensions, design and installation guidelines, International Organization for Standardization, 1995.
[33] Standards Australia, AS 3634-1989 (R2013) - Solar heating systems for swimming pools Standards Australia, SAI Global, 2013.
[34] M. Kovarik, P. Lesse, Optimal control of flow in low temperature solar heat collector, Solar Energy 18 (1976) 431-435.
[35] R. Winn, C. Winn, Optimal control of mass flow rates in flat plate solar collectors, ASME, Transactions, Journal of Solar Energy Engineering 103 (1981) 113-120.
[36] V. Badescu, Optimal control of flow in solar collectors for maximum exergy extraction, International journal of heat and mass transfer 50 (2007) 4311-4322.
[37] J. Yazdanpanahi, F. Sarhaddi, M. Mahdavi Adeli, Experimental investigation of exergy efficiency of a solar photovoltaic thermal (PVT) water collector based on exergy losses, Solar Energy 118 (2015) 197-208.
[38] Y.A. Cengel, J.M. Cimbala, Fluid mechanics: fundamentals and applications, 2nd ed ed., Boston, McGraw-Hill Higher Education, 2010.
[39] M. Farshchimonfared, J.I. Bilbao, A.B. Sproul, Full optimisation and sensitivity analysis of a photovoltaic–thermal (PV/T) air system linked to a typical residential building, Solar Energy 136 (2016) 15-22.
[40] S.M. Bambrook, A.B. Sproul, Maximising the energy output of a PVT air system, Solar Energy 86 (2012) 1857-1871.
[41] J.I. Bilbao, A.B. Sproul, Detailed PVT-water model for transient analysis using RC networks, Solar Energy 115 (2015) 680-693.
[42] M. Martin, P. Berdahl, Characteristics of infrared sky radiation in the United States, Solar Energy 33 (1984) 321-336.
[43] W.H. McAdams, Heat transmission. McGraw-Hill New York, 1954.
[44] F. Test, R. Lessmann, A. Johary, Heat transfer during wind flow over rectangular bodies in the natural environment, Journal of Heat Transfer 103 (1981) 262-267.
[45] S. Sharples, P. Charlesworth, Full-scale measurements of wind-induced convective heat transfer from a roof-mounted flat plate solar collector, Solar Energy 62 (1998) 69-77.
[46] J.I. Bilbao, Photovoltaic thermal water Systems - modelling and design considerations for residential applications in different climates and demand conditions, Ph.D. Thesis, University of New South Wales, 2012.
[47] A. Buonomano, G. De Luca, R.D. Figaj, L. Vanoli, Dynamic simulation and thermo-economic analysis of a PhotoVoltaic/Thermal collector heating system for an indoor–outdoor swimming pool, Energy Conversion and Management 99 (2015) 176-192.

[48] J.C. Lam, W.W. Chan, Life cycle energy cost analysis of heat pump application for hotel swimming pools, Energy Conversion and Management 42 (2001) 1299-1306.
[49] E. Ruiz, P.J. Martínez, Analysis of an open-air swimming pool solar heating system by using an experimentally validated TRNSYS model, Solar Energy 84 (2010) 116-123.
[50] D. Richter, Temperatur- und Wärmehaushalt des thermisch belasteten Stechlin- und Nehmitzsees Abhandlung des Meteorologischen Dienstes Akademie-Verlag, Berlin Nr.123, (1979)
[51] ISO, ISO 9806:2013 (E) Solar energy - Solar thermal collectors - Test methods, International Organization for Standardization, 2013.
[52] J. Taylor, Introduction to error analysis, the study of uncertainties in physical measurements. Vol. 1. University Science Books,U.S., 1997.
[53] AstralPool, E-series Pump. Technical specifications. https://www.astralpool.com.au/products/pumps/eseriespump, 2018 (accessed 2018 January 29th).
[54] A. Walker, Solar Energy: Technologies and project delivery for buildings. John Wiley & Sons, 2013.
[55] J. Gordon, Solar energy: the state of the art: ISES position papers. Earthscan, 2001.
[56] The Engineering ToolBox, PE - PolyEthylene Pipes, Flow and Pressure Loss. http://www.engineeringtoolbox.com/pe-pipe-pressure-loss-d_619.html, 2016 (accessed 2016 January 5th).
[57] C. Vasile, M. Pascu, Practical guide to polyethylene. iSmithers Rapra Publishing, 2005.
[58] W.M. Kays, M.E. Crawford, B. Weigand, Convective heat and mass transfer. Tata McGraw-Hill Education, 2012.
[59] DOE, M&V Guidelines: Measurement and Verification for Performance-Based Contracts Version 4.0, Prepared for the U.S. Department of Energy Federal Energy Management Program, Office of Energy Efficiency & Renewable Energy, U.S. Department of Energy, 2015.
[60] W. McMillan, Heat dispersal – Lake Trawsfynydd cooling studies. In: Symposium on Freshwater Biology and Electrical Power Generation, Part 1, (1971) 41-80.
[61] C.C. Smith, G. Löf, R. Jones, Measurement and analysis of evaporation from an inactive outdoor swimming pool, Solar Energy 53 (1994) 3-7.
[62] C. Rohwer, Evaporation from free water surfaces. US Department of Agriculture, 1931.
[63] ASHRAE, ASHRAE handbook. Applications. Atlanta, GA : American Society of Heating, Refrigerating and Air-Conditioning Engineers, 2003.
[64] BOM, Terrey Hills, New South Wales - Daily Weather Observations. Bureau of Meteorology, Australia Government. http://www.bom.gov.au/climate/dwo/IDCJDW2154.latest.shtml, 2018 (accessed 2019 January 15th).
[65] Solar Energy Laboratory, TRNSYS 17, A transient systems simulation program., 2011.
[66] DOE, Managing Swimming Pool Temperature for Energy Efficiency. Office of Energy Efficiency & Renewable Energy, U.S. Department of Energy. http://energy.gov/energysaver/managing-swimming-pool-temperature-energy-efficiency, 2016 (accessed 2016 July 6th ).
[67] Energy Australia, Ausgrid zone: Basic Home (Standing Offer Tariff) - Peak Only. Energy Price Fact Sheet NSW Residential (Electricity). https://secure.energyaustralia.com.au/EnergyPriceFactSheets/PricingFactSheets.aspx, 2018 (accessed 2018 February 10th ).
[68] DEE, National Greenhouse Accounts Factors, Department of the Environment and Energy, Commonwealth of Australia, 2018.
[69] Rheem Pool Heating, About heat pumps: Operating Characteristics. http://www.rheempoolheating.com.au/page/about_heat_pumps.html, 2016 (accessed 2016 January 10th).